

Hydrodynamic characteristics of Tapered Fluidized bed in Ternary mixture using Artificial Neural Network

Thesis submitted

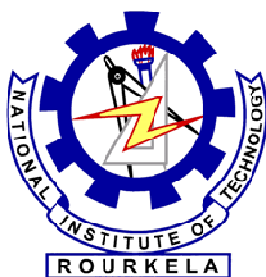
By

KONDURU PRADEEP KUMAR (209CH1056)

In partial fulfillment for the award of the Degree of
Master of Technology

In

Chemical Engineering



Department of Chemical Engineering
National Institute of Technology
Rourkela-769008, Orissa, India
May, 2011

Hydrodynamic characteristics of Tapered Fluidized bed in Ternary mixture using Artificial Neural Network

THESIS SUBMITTED

by

KONDURU PRADEEP KUMAR (209CH1056)

In partial fulfillment for the award of the Degree of

MASTER OF TECHNOLOGY

IN

CHEMICAL ENGINEERING

Under the esteemed guidance of

Prof. K.C.BISWAL



DEPARTMENT OF CHEMICAL ENGINEERING

NATIONAL INSTITUTE OF TECHNOLOGY, ROURKELA-769008.

ORISSA, INDIA 769008

May – 2011

**National Institute of Technology
Rourkela**



CERTIFICATE

This is to certify that the thesis entitled, “**Hydrodynamic characteristics of Tapered Fluidized bed in Ternary mixture using Artificial Neural Network**” submitted by Sri KONDURU PRADEEP KUMAR in partial fulfillments for the requirements for the award of Master of Technology Degree in Chemical Engineering Department at National Institute of Technology, Rourkela (Deemed University) is an authentic work carried out by him under my supervision and guidance.

To the best of my knowledge, the matter embodied in the thesis has not been submitted to any other University / Institute for the award of any Degree or Diploma.

Date:

Prof. K.C.BISWAL

Dept.of Chemical Engineering
National Institute of Technology
Rourkela - 769008

ACKNOWLEDGEMENTS

I am grateful to our supervisor, Prof. K.C.Biswal, for his kind support, guidance and encouragement throughout the project work, also for introducing to this topic.

I express my gratitude and indebtedness to Dr. A.Sahoo, Dr. M.Kundu, Dr. B.Munshi , Dr. Santanu Paria, Dr. S.Mishra and Dr. S.Khanam for their valuable suggestions and instructions at various stages of the work.

I express my immense gratitude to Professor G.K.Roy of the Department of Chemical Engineering for his valuable suggestions and encouragement.

I would like to express my appreciation to all those people especially Seshu, Jeevan, Yoganand and my class mates who have contributed to make this work possible through their help and support along the way.

Finally, I express my thankful to Lab Technicians, for his support at all stages.

Place:

Date:

KONDURU PRADEEP KUMAR
(209CH1056)

Contents

Particulars	Page No
Abstract	I
List of figures	II
List of tables	IV
Nomenclature	V
1. Introduction	1
2. Literature review	4
2.1 Phenomenon of fluidization	5
2.2 Experimental phenomena	6
2.3 Mathematical development of model	7
2.4 Development of correlations for bed fluctuation ratio 'r'	9
2.5. Development of correlations for bed expansion ratio 'R'	11
3 Experimental setup and procedure	12
4 Development of correlations	17
4.1 Dimensional analysis	18
4.2 Artificial neural network	19
5 Results and discussion	21
5.1. Study of minimum fluidization velocity (U_{mf}) and pressure drop (ΔP_{mf}) at minimum fluidization	22
5.2. Study of bed fluctuation ratio 'r'	25
5.3. Study of bed expansion ratio 'R'	27

5.4. Development of correlations for bed fluctuation ratio by dimensional analysis (DA)	29
5.5. Development of correlations for bed expansion ratio by dimensional analysis (DA)	33
5.6. Development of correlations of 'r' and 'R' by artificial neural network (ANN) approach	37
6 conclusion	40
References	42
Appendix	45

Abstract

Tapered beds are extensively used in various industrial chemical processes. These beds are remedy for certain drawbacks of the gas-solid system. To study the hydrodynamic characteristics of homogeneous ternary mixtures, several experiments have been carried out for glass beads as a material with different compositions of various sizes of particles. The correlations for bed expansion ratio and fluctuation ratio are developed using system parameters as initial static bed height, average particle diameter and superficial gas velocity by dimensionless analysis. The experimental values are compared with correlations developed by Artificial Neural Network (ANN) and Dimensional Analysis (DA) approach. The correlations obtained by ANN and DA are agreed well with experimental values..

List of Figures

Fig No	Title	Page no
2.1	Effect of Superficial gas velocity (U_{g0}) on total pressure drop (ΔP_t).	7
2.2	Structure of the bed	8
3.1	Line diagram of hydrodynamic characteristics of tapered bed.	13
3.2	The experimental set-up for hydrodynamics study of gas-solid fluidization of a ternary mixture in a tapered bed.	13
4.1	Illustration of ANN	19
5.1	Variation of bed pressure drop with superficial gas velocity for cone angle of 7.47° and with equal mixtures for different H_s .	22
5.2	Variation of bed pressure drop with superficial gas velocity for cone angle of 11.2° and $H_s=9.5\text{cm}$ for different mixtures.	23
5.3	Variation of bed pressure drop with static bed height for varying superficial gas velocity of const. mixture 20:20:60 and for cone angle of 4.61°	23
5.4	Variation of bed pressure drop with gas superficial velocity for varying cone angles of const. $H_s=10.5\text{ cm}$ and equal mixture.	24
5.5	Variation of bed fluctuation ratio with superficial gas velocity for cone angle of 4.61° and for a mixture of 40:30:30 for different H_s .	25
5.6	Variation of bed fluctuation ratio with superficial gas velocity for cone angle of 4.61° and $H_s=12\text{cm}$ for different mixtures.	25
5.7	Variation of bed fluctuation ratio with static bed height for varying superficial gas velocity of const. mixture 40:30:30 and for cone angle of 4.61°	26
5.8	Variation of bed fluctuation ratio with gas superficial velocity for varying cone angles of const. $H_s=10.5\text{ cm}$ and for a mixture of 20:60:20.	26
5.9	Variation of bed expansion ratio with superficial gas velocity for cone angle of 7.47° and for a mixture of 20:60:20 for different H_s .	27
5.10	Variation of bed expansion ratio with superficial gas velocity for cone angle of 11.2° and $H_s=8.5\text{ cm}$ for different mixtures.	28
5.11	Variation of bed expansion ratio with static bed height for varying superficial gas velocity of const. mixture 40:30:30 and for cone angle of 4.61° .	28
5.12	Variation of bed expansion ratio with gas superficial velocity for varying cone angles of const. $H_s=10.5\text{ cm}$ and for a mixture of 20:60:20.	29

5.13	Plot of r vs $(G_m - G_{mf})/G_{mf}$.	30
5.14	Plot of r vs D_o/D_{psm} .	30
5.15	Plot of r vs. H_s/D_0 .	31
5.16	Plot of r Vs $\tan \alpha$	31
5.17	Plot of r vs. r product	32
5.18	Plot of r cal vs. r exp.	32
5.19	Plot of R vs $(G_m - G_{mf})/G_{mf}$.	33
5.20	Plot of R vs D_o/D_{psm} .	34
5.21	Plot of R vs. H_s/D_0 .	34
5.22	Plot of R Vs $\tan \alpha$.	35
5.23	Plot of R vs. R product.	35
5.24	Plot of R cal vs. R exp.	36
5.25	Performance plot for r .	37
5.26	Performance plot for R .	38
5.27	Comparison of experimental and calculated values of r by both DA and ANN approaches.	38
5.28	Comparison of experimental and calculated values of r by both DA and ANN approaches	39

List of Tables

Table No	Title	Page no
2.1	Various types of bed and its correlation coefficients (K, a, b and c) for 'r'.	11
2.2	Various types of bed and its correlation coefficients (K, a, b and c) for 'R'.	11
3.1	Material properties.	16
4.1	Experimental data used for development of correlations by DA.	18
4.2	ANN parameters.	20
5.1	Deviations of r and R.	36
5.2	Deviations of r and R by experimental with calculated values of r and R by DA and ANN approaches.	39

Nomenclature

D_0	: Bottom diameter of tapered bed, m.
D_1	: Top diameter of tapered bed, m.
D_c	: Mean diameter of tapered bed, m.
dp	: Particle diameter, m.
dp_{sm}	: Average mean particle diameter, m.
h_s	: Static bed height, m.
U	: Superficial velocity of fluid, m/sec.
U_{mf}	: Minimum fluidization velocity or critical fluidization velocity, m/sec.
G	: Flow rate of fluid at fluidization condition, m^3/hr .
G_f or G_{mf}	: Flow rate of fluid at minimum fluidization condition, m^3/hr .
r	: Bed fluctuation ratio
R	: Bed expansion ratio
g	: Acceleration due to gravity, m/sec^2 .
ΔP_{mf}	: Pressure drop at minimum fluidization condition, N/m^2

Greek letters

ρ_f	: Fluid density, Kg/m^3 .
α	: Tapered angle, deg.
μ_f	: Fluid viscosity, $kg/m\cdot sec$.
ρ_{sm}	: Density of mixture, Kg/m^3 .

Subscripts

mf	: Minimum fluidization
f	: Fluid
c	: Critical
s	: Static or stagnant

Chapter 1

Introduction

INTRODUCTION:

Fluidization is an established fluid-solid contacting technique, which finds massive applications in combustion, gasification, carbonization, drying of solids, coating of particles, incineration of waste materials, liquefaction and many others. Apart from the various advantages, the efficiency and quality of fluidization is adversely affected [1]. In cylindrical beds, the particle size reduction results in entrainment, limitation of operating velocity in addition to other demerits like slugging, non-uniform fluidization allied with such beds [2]. Various techniques including introducing of baffles, operation in multistage units, imparting vibrations and alteration in bed geometry have been advocated from time to time to tackle the problems [3]. These disadvantages can be overcome by the use of tapered fluidized beds in which superficial gas velocity of the fluid gradually reduces with height due to increase in cross-sectional area. Tapered fluidized beds have found wide applicability in many industrial processes such as biological treatment of waste water [4], metabolic gas production [5], immobilized bio-film reaction, incineration of waste materials, coating of nuclear fuel particles, roasting sulfide ores, crystallization, coal gasification and liquefaction and food processing [6,7]. These beds are also useful for fluidization of materials with wide particle size distribution and for exothermic reactions. Due to angled wall, random and unrestricted particle movement occurs in tapered bed thereby reducing back mixing [8, 9].

Conical fluidized bed is very much useful for the fluidization of wide distribution of particles, since the cross sectional area is enlarged along the bed height from the bottom to the top, therefore the velocity of the fluidizing medium is relatively high at the bottom, ensuring fluidization of the large particles and relatively low at the top, preventing entrainment of the small particles. Since the velocity of fluidizing medium at the bottom is fairly high, this gives rise to low particle concentration, thus resulting in low reaction rate and reduced rate of heat release. Therefore the generation of high temperature zone near the distributor can be prevented. Due to the existence of a gas velocity gradient along the height of a conical bed, it has some favorable special hydrodynamics characteristics. The conical bed has been widely applied in many industrial processes such as,

1. Biological treatment of waste water,
2. Immobilized bio-film reaction,
3. Incineration of waste-materials,
4. Coating of nuclear fuel particles,
5. Crystallization, roasting of sulfide ores,
6. Coal gasification and liquefaction,
7. Catalytic polymerization,
8. Fluidized contactor for sawdust and mixtures of wood residues and
9. Fluidization of cohesive powder.

Several researchers have studied the hydrodynamic characteristics of homogeneous and heterogeneous systems of regular and irregular mixtures so far. A few reports were found regarding the use of Artificial Neural Networks (ANN) in hydrodynamic studies of binary systems. To the best of our knowledge, no literature was found concerning the application of ANN in hydrodynamic characteristics of ternary mixtures. In this work, an assay is made to develop the correlations for bed expansion ratio and fluctuation ratio using three layered ANN. The results obtained using ANN approach is promising.

Chapter 2

Literature Review

2.1 PHENOMENON OF FLUIDIZATION:

When allowing a fluid either gas or liquid in vertical direction through a bed of fine particles, at a low flow rate of fluid slightly penetrates through the void space between the stationary particles. This type of bed is known as fixed bed. With slight increase in flow rate, few particles seem to be vibrating in a bounded region. This type of bed is known as expanded bed. At a still higher velocity, the pressure drop in the bed increases up to a certain velocity and achieves a maximum pressure drop, at that point of velocity is known as critical fluidization velocity or minimum fluidization velocity. At this instant, particles at the bottom of bed begin to fluidize and force exerted between a particle and fluidizing medium counterbalances the effective weight of the particle. There after slight increase in a fluid the pressure drop falls sharply after that decreases slowly up to certain velocity, this is known as partially fluidized bed. Further increasing flow rate the pressure drop through the bed remains constant, this type of bed is known as fully fluidized bed or spouted bed. Gas–solid systems generally behave in pretty different manner. With an increase in flow rate beyond minimum fluidization, large instabilities with bubbling and channeling of gas are observed. At higher flow rates agitation becomes more violent and the movement of solids becomes vigorous. In addition, the bed does not expand much beyond its volume at minimum fluidization. Such a bed is called an aggregative fluidized bed, a heterogeneous fluidized bed, a bubbling fluidized bed, or simply a gas fluidized bed.

Kumar and Roy (2004) proposed a model for bed expansion ratio in a gas-solid fluidized bed with disk and blade promoters using Artificial Neural Network (ANN) approach Sahoo and Roy (2008) proposed a model based on segregation distance which refers the segregation characteristics for irregular binary mixtures of homogeneous and heterogeneous system with the system parameters as initial static bed height, average particle diameter, height of a layer particles above the bottom grid and superficial gas velocity using Artificial Neural Network (ANN) approach and Dimensional Analysis (DA) approach. Mohanty et al (2007, 2008 and 2009) was used to study the effect of rod and disc promoters on bed fluctuation and expansion ratio and the models are developed for bed expansion and fluctuation ratio with the effect of parameters as flow rate, static bed height, particle sizes and densities using Statistical (Factorial Design) and ANN approach.

2.2 EXPERIMENTAL PHENOMENA:

Flow Regimes:

A typical diagram of the hydrodynamic characteristics of the conical bed is shown in Fig.2.1 with the increase of superficial gas velocity (U_{g0}), the total pressure drop (ΔP_t), varies along the line of $O \rightarrow A \rightarrow B \rightarrow C$ as given by S. Jing et al [6]. In the different stages, the hydrodynamic characteristics of fluidization of the conical bed are as follows

O \rightarrow A stage:

Because U_{g0} is relatively low; the stagnant height of the particle bed remains unchanged as at the beginning. The total pressure drop, ΔP_t , increases up to the maximum point, ΔP_{max} , i.e. point A. This phenomenon is the same as that observed for liquid–solid tapered beds by Peng and Fan [7], and the flow regime is also termed the fixed bed regime. The superficial gas velocity, to which point A in Fig.2.1 corresponds, is called the minimum fluidized velocity, U_{mf} .

A \rightarrow B stage:

When U_{g0} is higher than U_{mf} , ΔP_t decreases with the increase of U_{g0} , and it is observed that the stagnant height of the conical bed does not change. The same phenomenon is also observed for gas–solid systems by Olazar et al. [16] and for liquid–solid systems by Peng and Fan [7]. Here, the flow regime is named a partially fluidized bed. When U_{g0} reaches U_{ms} , the characteristics of total pressure drop are different from those in the above two stages.

B \rightarrow C stage:

If U_{g0} is greater than U_{ms} , ΔP_t stays nearly constant as shown in below Fig. In this stage, it is observed that slugging fluidization, bubble fluidization and spouting fluidization occur for the conical bed. In this stage, the characteristics of fluidization of the gas–solid conical bed are different from that of liquid–solid ones as reported by Peng and Fan [7]. Depending on the cone angle, the flow regime is called a slugging or spouting fluidization regime.

Reversing the fluidization process, the fluidized bed is de-fluidized by decreasing the superficial gas velocity. The same regimes are observed in below Fig 2.1.

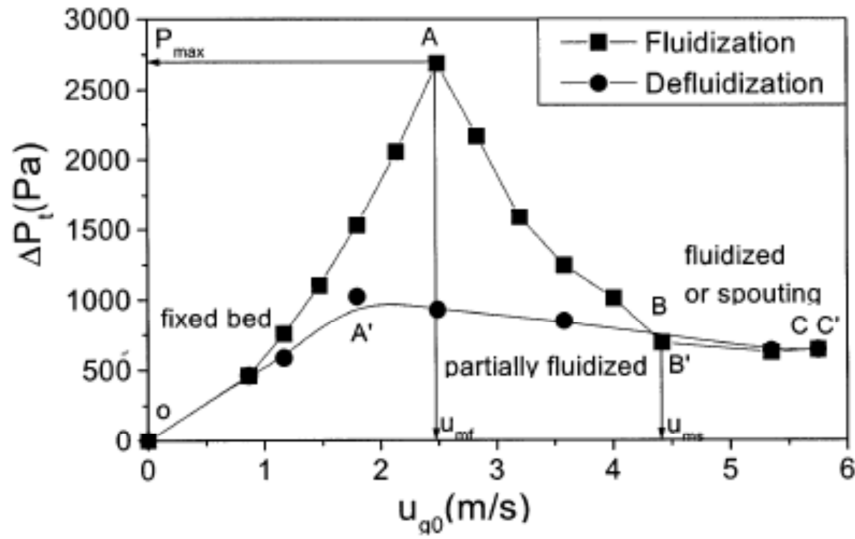


Fig 2.1. Effect of Superficial gas velocity (U_{g0}) on total pressure drop (ΔP_t).

2.3 MATHEMATICAL DEVELOPMENT OF MODEL:

In the course of experiments it has been observed that, at a particular velocity, the pressure drop reaches a maximum and the particles in the bed are lifted slightly upward by the fluid. This is followed by the particles at the bottom of the bed beginning to fluidize. Once the particles are unlocked there is a sharp decline in the pressure drop. Evidently, fluidization is initiated when the force exerted by the fluidizing medium flowing through the bed is equal to the total effective weight of the particles in the bed. It is assumed that the lateral velocity of the fluid is relatively small and can be neglected [17].

The pressure drop through a packed bed over a differential height of “dh” is given by Ergun [18] as follows

$$\frac{\Delta P}{H} = \frac{150U_{mf}\mu_g(1-\epsilon_{mf})^2}{\phi_s^2 dp_{sm}^2 \epsilon_{mf}^3} + \frac{1.75U_{mf}^2 \rho_g(1-\epsilon_{mf})}{\phi_s dp_{sm} \epsilon_{mf}^3}$$

$$\text{i.e } dp = (AU + BU^2) dh$$

$$\text{Where } A = \frac{150U_{mf}\mu_g(1-\epsilon_{mf})^2}{\phi_s^2 dp_{sm}^2 \epsilon_{mf}^3} \text{ and } B = \frac{1.75U_{mf}^2 \rho_g(1-\epsilon_{mf})}{\phi_s dp_{sm} \epsilon_{mf}^3}$$

The overall pressure drop across the bed height, H, is obtained by integrating Ergun equation

$$-\Delta P = \int_{h_0}^{H+h_0} -(dp) = \int_{h_0}^{H+h_0} (AU + BU^2)dh$$

For a conical bed with apex angle of α

$$\frac{U}{U_0} = \frac{D_0^2}{D^2}, \frac{D}{D_0} = \frac{h}{h_0} \text{ and } U = U_0 \frac{h_0^2}{h^2}$$

So the integrated Ergun equation becomes

$$-\Delta P = \int_{h_0}^{H+h_0} \left(AU_0 \frac{h_0^2}{h^2} + BU_0^2 \frac{h_0^4}{h^4} \right) dh$$

On integration we get

$$-\Delta P = AU_0 \frac{H \cdot h_0}{(H + h_0)} + \frac{BU_0^2 \cdot h_0}{3} \left[1 - \frac{h_0^3}{(H + h_0)^3} \right]$$

$$\text{Where } h_0 = \frac{D_0}{2 \tan(\alpha/2)}$$

The area of cross-section-of a conical bed increases continuously from the bottom to the top. So the force exerted by the fluidizing medium on the solid particles is not directly proportional to the pressure drop. The force in a differential bed height of dh is equal to the product of the pressure drop through it, $-(dp)$, and the cross sectional area

On integration for a conical bed, we get

$$G = \frac{K \left[(H + h_0)^3 - h_0^3 \right]}{3} = C$$

$$\text{Where } K = \frac{g(1 - \varepsilon)(\rho_s - \rho_f)\pi D_0^2}{4h_0^2}$$

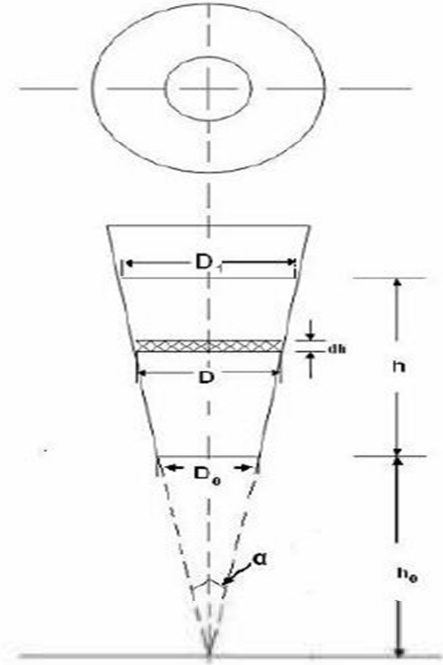


Figure 2.2 Structure of the bed

Now according to the proposed model as given by Agarwal and Roy [17], the particles at the bottom start fluidizing when $F=G$. therefore the minimum fluidization velocity, U_{mf} can be found out by equating $F=G$, that gives

$$A_1 U_{mf}^2 + B_1 U_{mf} = C_1$$

$$\text{Or } U_{mf} = \frac{-B_1 + \sqrt{B_1^2 + 4A_1 C_1}}{2A_1}$$

$$\text{Where } A_1 = \frac{\pi B D_0^3 H}{4(D_0 + 2H \tan \alpha/2)}, B_1 = \frac{\pi A D_0^2 H}{4} \text{ and } C_1 = \frac{K[(H + h_0)^3 - h_0^3]}{3}$$

Putting $U_o = U_{mf}$ at after coming of integrated Ergun equation we get

$$-(\Delta P_{mf}) = A H h_0 U_{mf} + \frac{B h_0 [(H + h_0)^3 - h_0^3] U_{mf}}{3(H + h_0)^3}$$

2.4 DEVELOPMENT OF CORRELATIONS FOR BED FLUCTUATION RATIO ‘r’:

For a gas flow more than the minimum fluidization velocity or critical fluidization velocity, the top of the fluidized bed may fluctuate significantly. The extent of the fluctuation and its estimation becomes important while specifying the height of a fluidizer. The fluctuation may be defined as the ratio of the highest and the lowest level of the top of the bed for any fluidizing gas mass velocity. This ratio is termed as the fluctuation ratio. Bed fluctuation and fluidization quality being inter-related, consistent efforts have been made to correlate fluctuation ratio in terms of static and dynamic parameters of the system.

By experimentally fluctuation ratio is

$$r = \frac{\text{highest level of bed raises } (h_{max})}{\text{lowest level of bed raises } (h_{min})}$$

A correlation for fluctuation ratio in conical vessels for regular particle has been developed by Biswal et al[19] using dimensional analysis approach based on four dimensionless groups neglecting the effect of density of gas and solid particles. The correlation reported by

Biswal et al [20] for fluctuation ratio of regular particle is given in equation (1) and for irregular particle is in equation (2).

$$r = 3.168 \left[\left(\frac{dp}{D_0} \right)^{0.14} \left(\frac{d_c}{h_s} \right)^{-0.16} \left(\frac{h_s}{D_0} \right)^{-0.24} \left(\frac{G_f - G_{mf}}{G_{mf}} \right)^{0.17} \right] \quad (1)$$

The bed fluctuation ratio for irregular particles in conical vessels is given by Biswal et al [19] as

$$r = 9.48 \left[\left(\frac{dp}{D_0} \right)^{0.27} \left(\frac{d_c}{h_s} \right)^{-0.83} \left(\frac{\rho_s}{\rho_f} \right)^{-0.15} \left(\frac{G_f - G_{mf}}{G_{mf}} \right)^{0.32} \right] \quad (2)$$

Another set of correlations given by Singh et al [21] for bed fluctuation ratio in conical conduits are,

For heterogeneous and spherical particles:-

$$r = 0.44 \left(\frac{G_f}{G_{mf}} \right)^{0.58} \left(\frac{\rho_{sm}}{\rho_f} \right)^{-0.1} \left(\frac{D_p}{D_0} \right)^{-0.06} (\tan \alpha)^{-0.17}$$

For non-spherical particles:-

$$r = 3.42 \left(\frac{G_f - G_{mf}}{G_{mf}} \right)^{-0.02} \left(\frac{D_0}{dp_{sm}} \right)^{-0.18} \left(\frac{h_s}{D_0} \right)^{0.033} \left(\frac{\rho_{sm}}{\rho_f} \right)^{-0.023}$$

For homogeneous and spherical particles:-

$$r = 9.8 \times 10^{-2} \left(\frac{G_f}{G_{mf}} \right)^{1.068} \left(\frac{D_0}{dp_{sm}} \right)^{-1.97} \left(\frac{h_s}{D_0} \right)^{-0.25} (\tan \alpha)^{-0.25}$$

For any bed the general form for the bed fluctuation ratio is given by Singh et al [22, 23],

$$r = K \left(\frac{d_p}{d_c} \right)^a \left[\left(\frac{d_c}{h_s} \right) \left(\frac{\rho_f}{\rho_s} \right) \right]^b \left(\frac{G_f - G_{mf}}{G_{mf}} \right)^c$$

Table 2.1. Various types of bed and its correlation coefficients (K, a, b and c) for 'r'.

Type of bed	K	a	b	c
Cylindrical	1.92	0.04	0.04	0.05
Semi cylindrical	2.32	0.05	0.04	0.07
Hexagonal	2.3	0.06	0.05	0.06
Square	2.5	0.09	0.04	-

2.5. DEVELOPMENT OF CORRELATIONS FOR BED EXPANSION RATIO 'R':

Expansion of gas-solid fluidized beds may in general result from the volume occupied by bubbles and from increase in voidage of the dense phase. It is given by the expression,

$$R = \frac{h_{max} + h_{min}}{2h_s} = \frac{h_{avg}}{h_s}$$

For any bed the general form for the bed expansion ratio is given by Singh et al [22, 23] as

$$R = K \left(\frac{d_p}{d_c} \right)^a \left(\frac{d_c}{h_s} \right)^b \left(\frac{G_f - G_{mf}}{G_{mf}} \right)^c$$

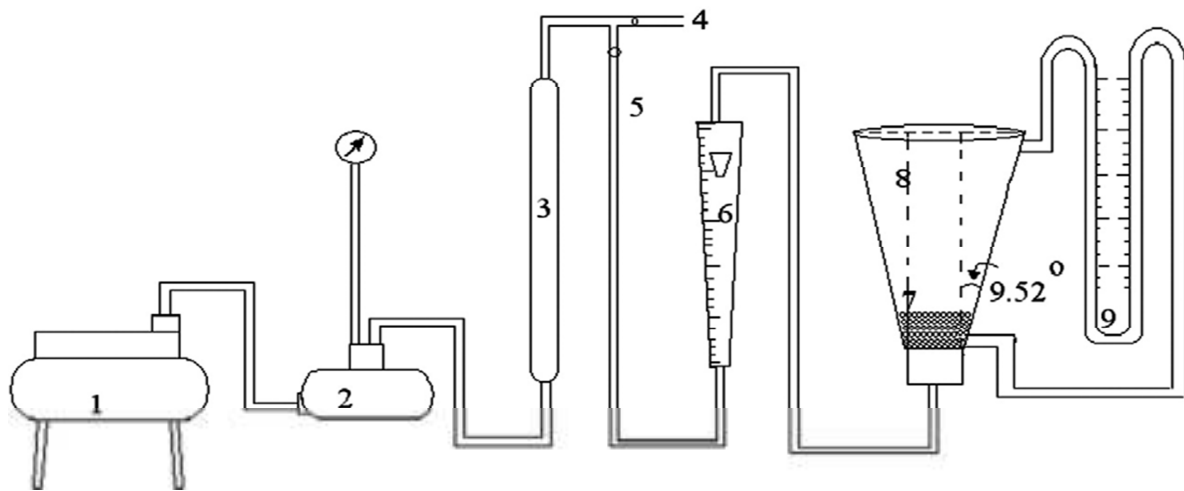
Table 2.2. Various types of bed and its correlation coefficients (K, a, b and c) for 'R'.

Type of bed		K	a	b	c
Non-spherical	Cylindrical	2.55	0.11	0.727	0.433
	Semi cylindrical	5.46	0.26	0.03	0.21
	Hexagonal	2.422	0.12		0.35
	Square	6.09	0.24		0.27
Spherical	Semi cylindrical	2.92	0.14	0.36	0.16
	Hexagonal	2.82	0.13		0.22

Chapter 3

Experimental Setup and procedure

EXPERIMENTAL SETUP:



1. Compressor 2. Receiver 3. Silica gel tower 4. Bypass valve 5. Line valve 6. Rotameter 7. Bed materials 8. Tapered bed 9. U-tube manometer

Figure 3.1. Line diagram of hydrodynamic characteristics of tapered bed.



Figure 3.2. The experimental set-up for hydrodynamics study of gas-solid fluidization of a ternary mixture in a tapered bed.

Experimental setup consists of air compressor, receiver, silica gel tower, by pass valve, line valve, rotameter, bed materials, fluidizer and U-tube manometer.

Air Compressor:

It is a multistage air compressor having sufficient capacity and it is used to takes the air from the atmosphere and compresses the air and it is stored in receiver.

Receiver:

It is horizontal cylinder used for storing the compressed air from compressor. There is one G.I. pipe inlet to the accumulator and one by-pass from one end of the cylinder. The exit line also at G.I line taken from the central port of the cylinder. The purpose for using air accumulator in the line is to dampen the pressure fluctuations. The accumulator is fitted with a pressure gauge; the operating pressure in the cylinder is kept at 20psig.

Silica gel tower:

A silica gel tower is provided in the line immediately after the receiver to remove the moisture content presented in air from the compressor.

Rotameter:

Rotameter is used for the measure flow rate of air. Two rotameters are fixed; one for the lower range (0-20 m³/hr) and the other for the higher range (20-120 m³/hr) were used to measure the air flow rates.

Air Distributor:

A 60 mesh screen at the bottom served as the support as well as the distributor. The distributor is an integral part of calming section where it is followed by a conical section [24]. The inside hollow space of the distributor filled with glass beads of 1.5 cm outer diameter, for uniform air distribution.

Tapered bed:

The tapered columns were made of Perspex sheets to allow visual observation with different tapered angles (4.61⁰, 7.47⁰, 9.52⁰ and 11.2⁰). Two pressure tapings are provided for noting the bed pressure drop.

Control valve:

A globe valve of 1.25cm inner diameter attached to next to the pressure gauge for sudden release of the line pressure. A gate valve of 15mm inner diameter is provided in the line to control the airflow to the bed.

U-tube manometer:

One set of manometer is arranged in this panel board to measure the pressure drop. Carbon tetrachloride (density= 1584 kg/m^3) is used as manometer liquid.

PROCEDURE:

The experiments were carried out in different columns having tapered angles of 4.61° , 7.47° and 9.52° and 11.2° . Three closely sieved samples of glass beads (density= 2600 kg/m^3) were used for the investigation. For ternary mixture, fairly good mixing has been achieved by coning and quartering method as done in experimental practice and classification has been avoided since the ratio of the largest to the smallest particle size in the mixture is kept below 2.3. Details of the tapered columns are given in Table 3.1. The densities of the particles were obtained by dividing the weight of the particles by the displaced water volume, when the particles were put into a cylindrical column filled with water.

The above three particle sizes have been mixed in the ratio of 40:30:30, 33.3:33.3:33.3, 20:60:20 and 20:20:60. The weighed quantity of each solid material of the mixture was poured into the fluidization column. Prior to recording any data the charge was vigorously fluidized with air at a velocity at which entrainment was not observed. After a certain time, the air flow was suddenly stopped to obtain mixed packed bed and then the experiment was started. The initial static bed height was recorded. Then the velocity of the air was increased incrementally allowing sufficient time to each a steady state. The rotameter and manometer readings were noted for each increment in flow rate from which superficial gas velocities and pressure drops were calculated. The velocity, at which the pressure drop was maximum, was taken as the critical fluidization velocity. The same process was repeated for different initial static bed heights, different mixture of particles and different tapered angles of the tapered beds.

Table 3.1. Material properties.

(A) Properties of bed material				(B) Mixture properties of ternary		
materials	Particle size (mm)	ρ_s (Kg/m ³)	Particle size ratio		composition	Avg particle dia (mm)
Glass beads (dp_1)	3.67	2600	$dp_1/dp_2=1.408$	Mixture-1	40:30:30	2.924
Glass beads (dp_2)	2.61	2600	$Dp_2/dp_3=1.169$	Mixture-2	33.3:33.3:33.3	2.841
Glass beads (dp_3)	2.234	2600	$dp_1/dp_3=1.646$	Mixture-3	20:60:20	2.749
				Mixture-4	20:20:60	2.598

Chapter 4

Development of correlations

4.1 Dimensional Analysis:

Table 4.1. Experimental data used for development of correlations by DA.

$\frac{G_m - G_{mf}}{G_{mf}}$	$\frac{D_0}{D_{p_{sm}}}$	$\frac{h_s}{D_0}$	$\tan(\alpha)$	r exp	R Exp
0.1429	17.4609	2.2292	0.0807	1.0275	1.0327
0.2857	17.4609	2.2292	0.0807	1.0708	1.0935
0.4286	17.4609	2.2292	0.0807	1.1404	1.1402
0.5714	17.4609	2.2292	0.0807	1.1897	1.1869
0.7143	17.4609	2.2292	0.0807	1.2222	1.2150
0.8571	17.4609	2.2292	0.0807	1.3109	1.2850
1.0000	17.4609	2.2292	0.0807	1.3471	1.3271
0.1111	16.4145	3.1667	0.0807	1.0128	1.0329
0.1111	17.4609	3.0625	0.0807	1.0168	1.0720
0.1111	18.4758	2.8750	0.0807	1.0194	1.1593
0.1429	18.4750	2.0833	0.0807	1.0571	1.0800
0.1429	18.4750	2.5000	0.0807	1.0323	1.0500
0.1429	18.4750	2.8125	0.0807	1.0072	1.0259
0.3750	16.8975	2.5000	0.0807	1.1053	1.1892
0.4167	16.1663	2.5000	0.1312	1.0943	1.1684
0.3846	16.7334	2.5000	0.1981	1.0860	1.1391

Using Dimensional Analysis a correlations are made with system parameters as Initial static bed height, average particle diameter, superficial gas velocity, tapered angle. The general form of the developed correlations for bed fluctuation ratio and expansion ratio can be represented as

$$r = K \left(\frac{G_m - G_{mf}}{G_{mf}} \right)^a \left(\frac{D_o}{D_{psm}} \right)^b \left(\frac{H_s}{D_o} \right)^c \tan(\alpha)^d$$

$$R = K \left(\frac{G_m - G_{mf}}{G_{mf}} \right)^a \left(\frac{D_o}{D_{psm}} \right)^b \left(\frac{H_s}{D_o} \right)^c \tan(\alpha)^d$$

From the above equation the unknown variables i.e correlation coefficients K, a, b, c and d are calculated using dimensional analysis and those are obtained by plotting effect of parameters Vs bed fluctuation ratio and expansion ratio.

4.2 Artificial Neural Network:

Artificial Neural Network has been used to develop the correlations for bed expansion and fluctuation ratio. A feed forward back propagated ANN with three layers contained varying number of nodes in each layer depicted in fig. 4.1. Initial static bed height, average particle diameter, superficial gas velocity, tapered angle and fluctuation or expansion ratio have considered as the inputs for the ANN. The outputs considered are k, a, b, c and d. Once required inputs and outputs are supplied, ANN is ready to train. Levenberg-Marquardt back propagation has been used to train the ANN, as it is efficient training algorithm among all available algorithms. Virtually 416 datasets were used for training and the same numbers of datasets were used to test the created network. The network properties and training parameters are listed in table 4.1.

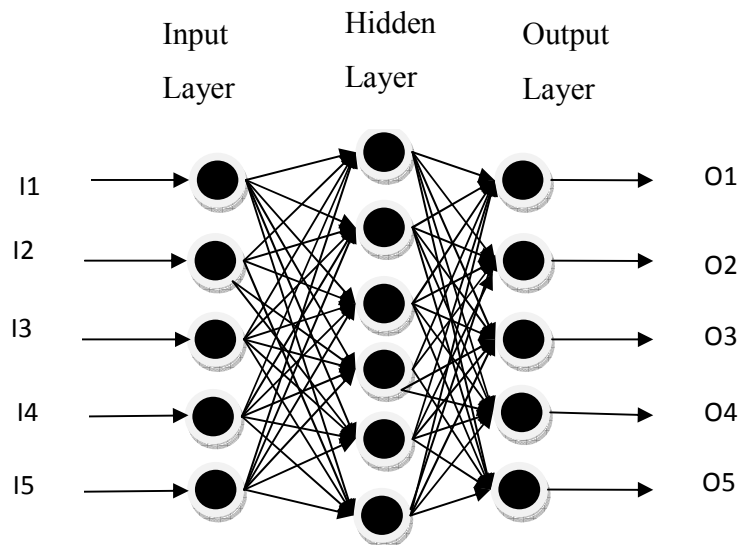


Fig.4.1 Illustration of ANN

Table 4.2 ANN parameters.

ANN Parameters	
Type	Three layered Feed forward back propagation
No of training datasets	416
No of testing datasets	416
Max cycles/epochs	1000
I/P Nodes	5
No of hidden nodes	6
No of O/P nodes	5

Chapter 5

Results and Discussion

5.1. STUDY OF MINIMUM FLUIDIZATION VELOCITY (U_{mf}) AND PRESSURE DROP (ΔP_{mf}) AT MINIMUM FLUIDIZATION:

The hydrodynamics characteristics of a tapered bed like U_{mf} & ΔP_{mf} is found to be a bit different from the conventional cylindrical beds. From the experimental observations given from Table A.1 to Table A.58 (refer appendix), the effects of the controlling variables like static bed height, average particle dia., gas velocity and tapered angle are studied.

(1) EFFECT OF STATIC BED HEIGHT (H_s):

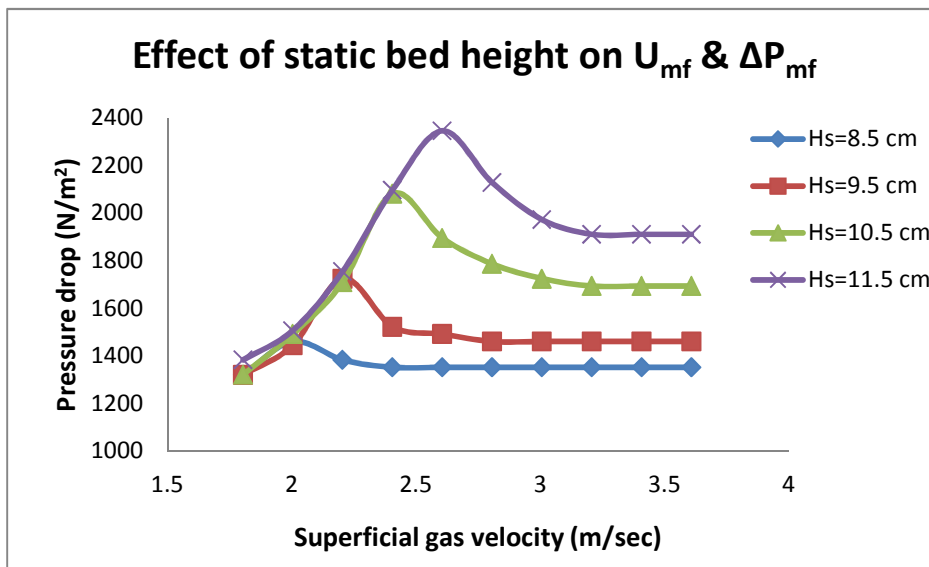


Fig 5.1. Variation of bed pressure drop with superficial gas velocity for cone angle of 7.47° and with equal mixtures for different H_s .

Discussion:

From the above graph it can be observe that there are three regimes namely fixed bed, partially fluidized and fully fluidized bed respectively, and the values of ΔP_{mf} and U_{mf} increase with increasing stagnant bed height (varying from 8.5 cm to 11.5 cm for mix of 33.3:33.3:33.3). Pressure drop occurs across the bed due to frictional resistance at particle surface and sudden expansion and contraction of flow through interstitials among the particles. It has a significant peak in minimum fluidization condition where bed changes from dormant state to homogeneous smoothly expanding condition.

(2) EFFECT OF AVERAGE PARTICLE DIAMETER ($D_{p_{sm}}$):

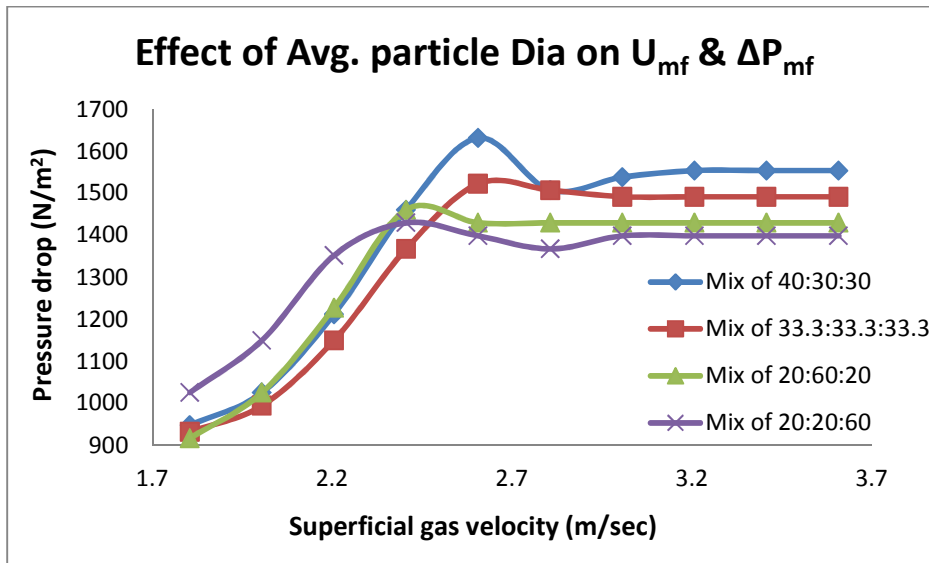


Fig 5.2. Variation of bed pressure drop with superficial gas velocity for cone angle of 11.2° and $H_s=9.5\text{cm}$ for different mixtures.

(3) EFFECT OF GAS VELOCITY:

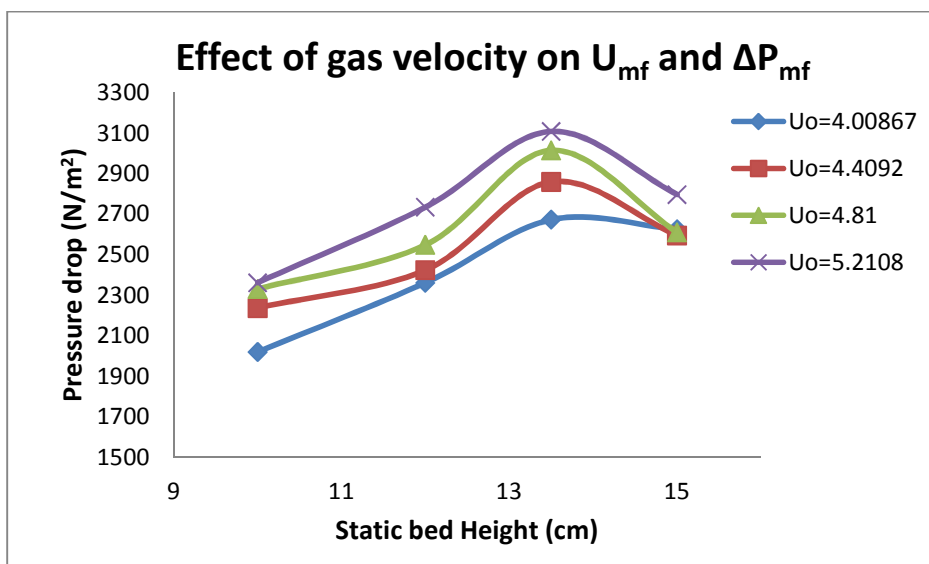


Fig 5.3. Variation of bed pressure drop with static bed height for varying superficial gas velocity of const. mixture 20:20:60 and for cone angle of 4.61°

(4) EFFECT OF TAPERED ANGLE (α):

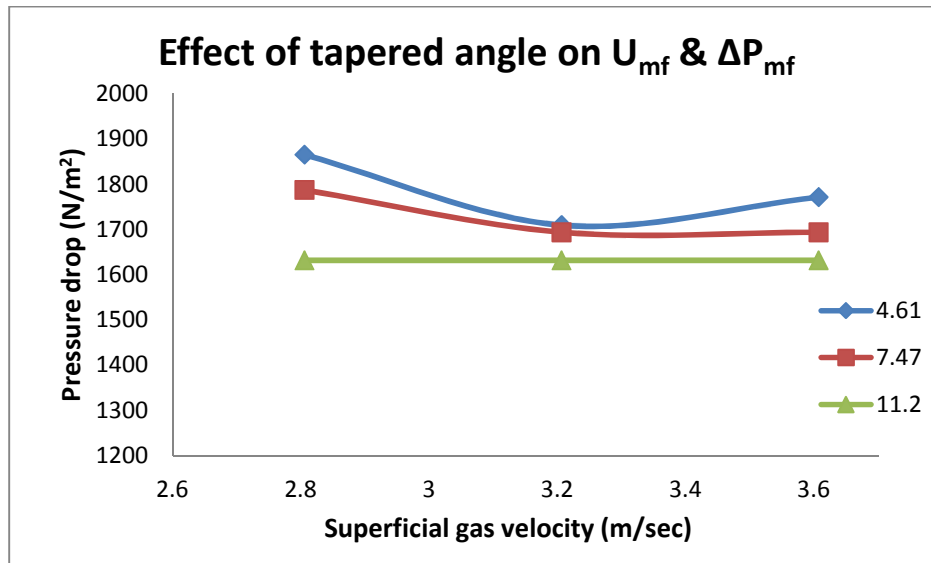


Fig 5.4. Variation of bed pressure drop with gas superficial velocity for varying cone angles of const. $H_s=10.5$ cm and equal mixture.

Discussion:

From the above graphs, both pressure drop and minimum fluidization velocity at minimum fluidization increases as increasing the average particle dia (i.e. decrease in percentage fines), and gas velocity. But for the tapered angle (apex angle) both pressure drop and minimum fluidization velocity decreases as increasing the tapered angle.

5.2. STUDY OF BED FLUCTUATION RATIO 'r':

(1) EFFECT OF STATIC BED HEIGHT (H_s):

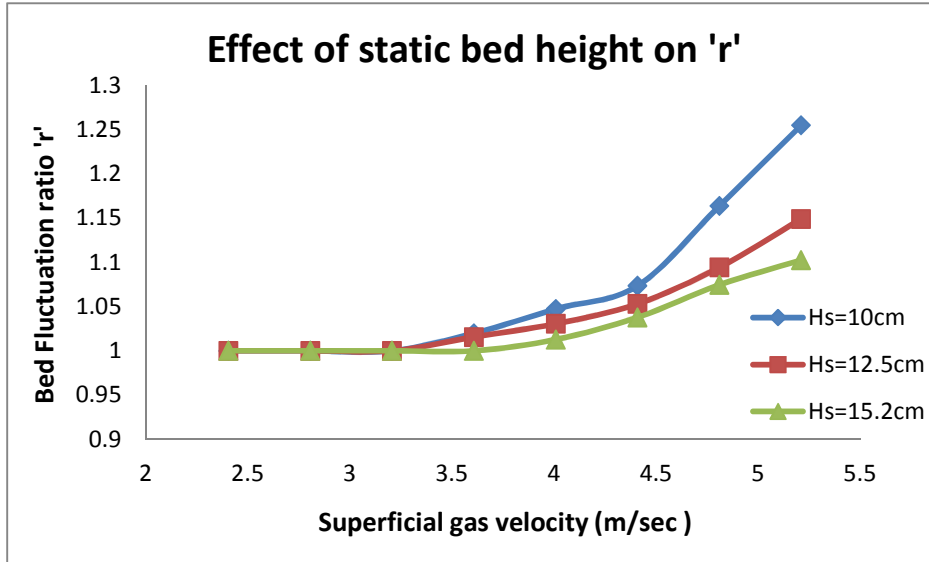


Fig 5.5. Variation of bed fluctuation ratio with superficial gas velocity for cone angle of 4.61° and for a mixture of 40:30:30 for different H_s .

(2) EFFECT OF AVERAGE PARTICLE DIAMETER ($D_{p_{sm}}$):

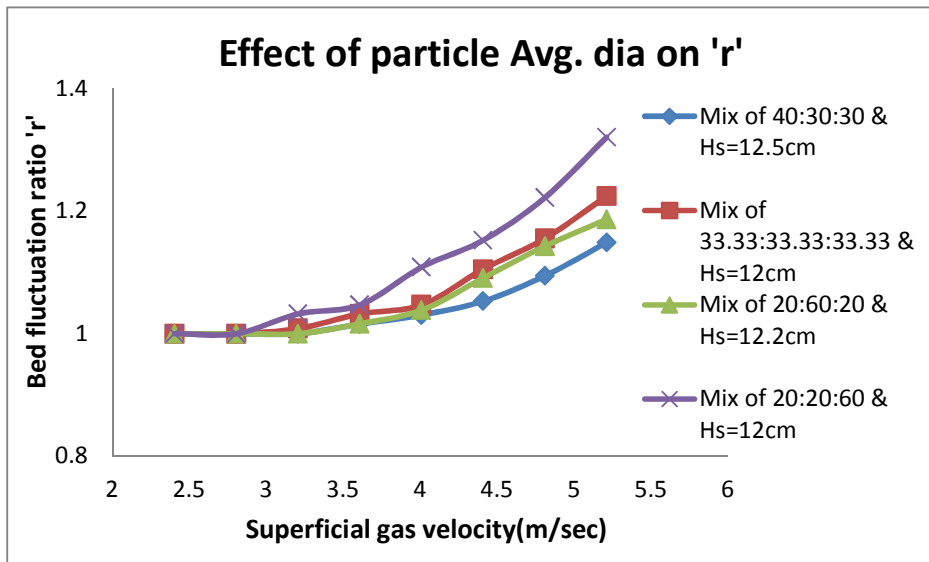


Fig 5.6. Variation of bed fluctuation ratio with superficial gas velocity for cone angle of 4.61° and $H_s \sim 12\text{cm}$ for different mixtures.

(3) EFFECT OF GAS VELOCITY:

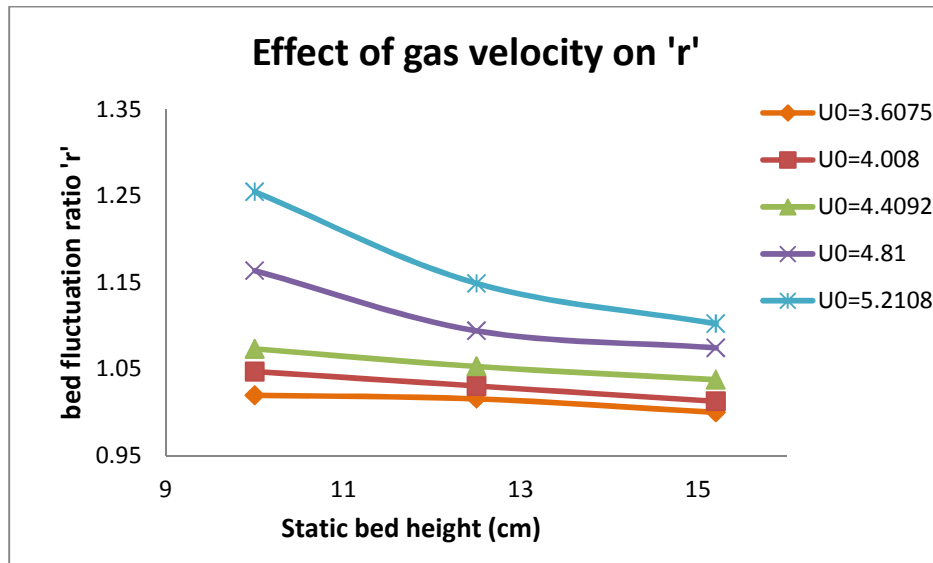


Fig 5.7. Variation of bed fluctuation ratio with static bed height for varying superficial gas velocity of const. mixture 40:30:30 and for cone angle of 4.61° .

(4) EFFECT OF TAPERED ANGLE (α):

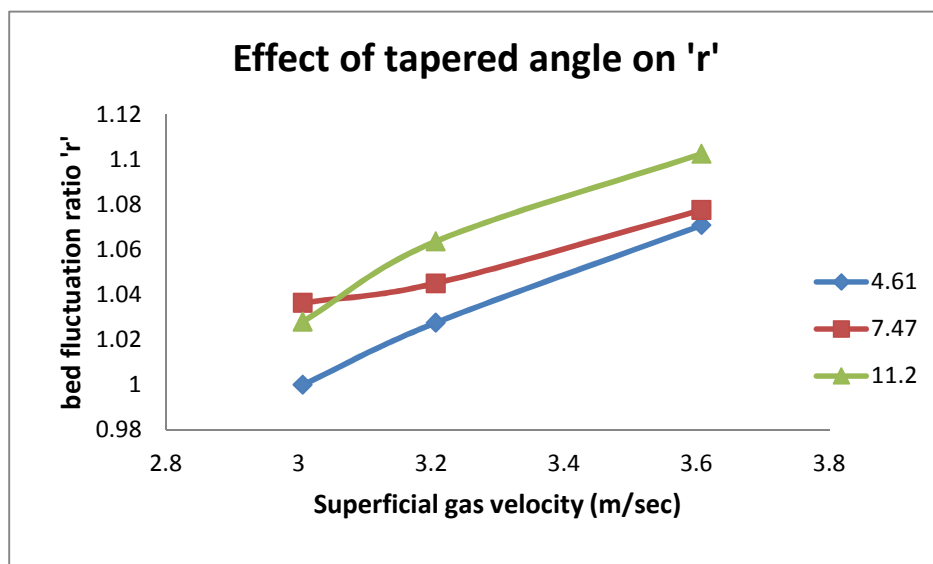


Fig 5.8. Variation of bed fluctuation ratio with gas superficial velocity for varying cone angles of const. $H_s=10.5$ cm and for a mixture of 20:60:20.

Discussion:

From the above figures, effect of parameters i.e average particle diameter, gas velocity and tapered angle increases, bed fluctuation ratio is also increases. But in the case of static bed height, as increases the bed height bed fluctuation ratio decreases.

5.3. STUDY OF BED EXPANSION RATIO 'R':

(1) EFFECT OF STATIC BED HEIGHT (H_s):

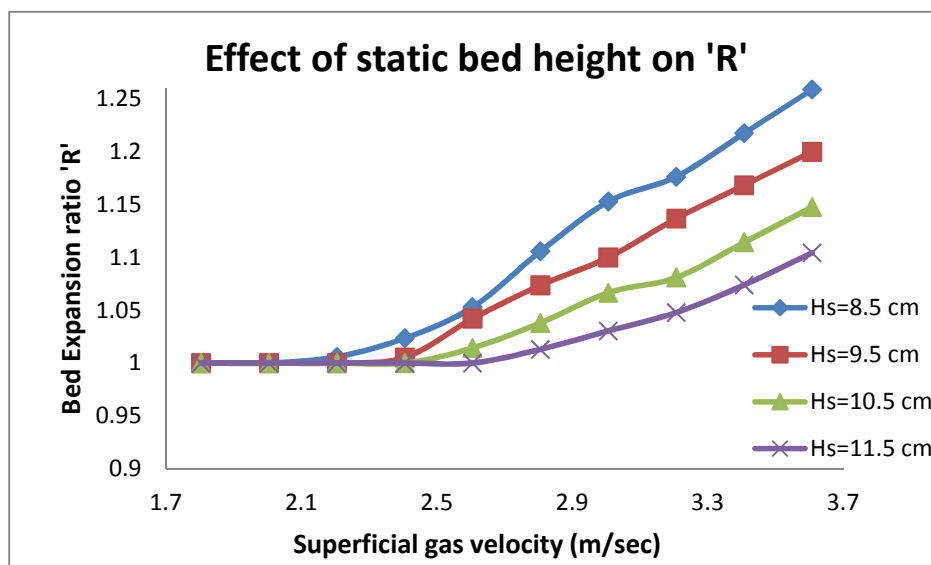


Fig 5.9. Variation of bed expansion ratio with superficial gas velocity for cone angle of 7.47° and for a mixture of 20:60:20 for different H_s .

(2) EFFECT OF AVERAGE PARTICLE DIAMETER ($D_{p_{sm}}$):

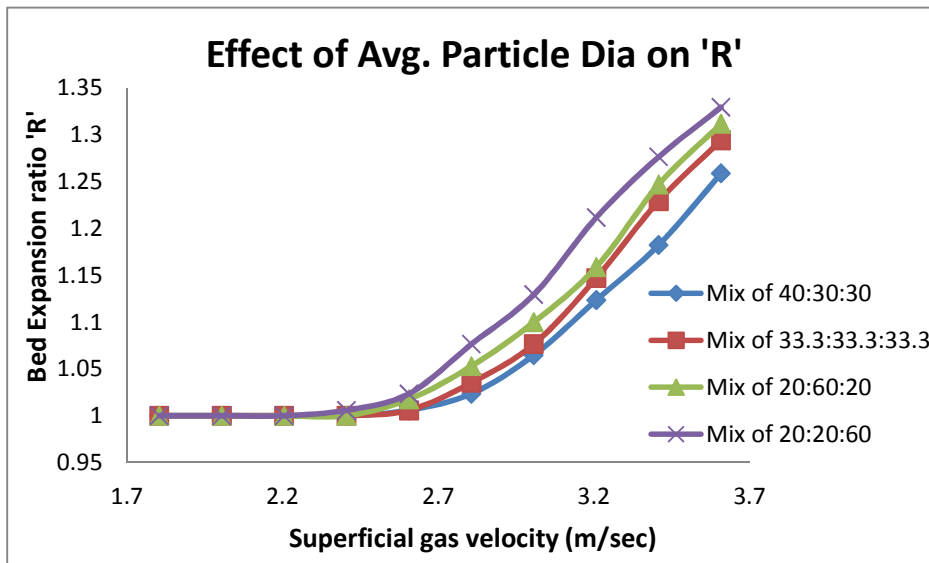


Fig 5.10. Variation of bed expansion ratio with superficial gas velocity for cone angle of 11.2° and $H_s=8.5$ cm for different mixtures.

(3) EFFECT OF GAS VELOCITY:

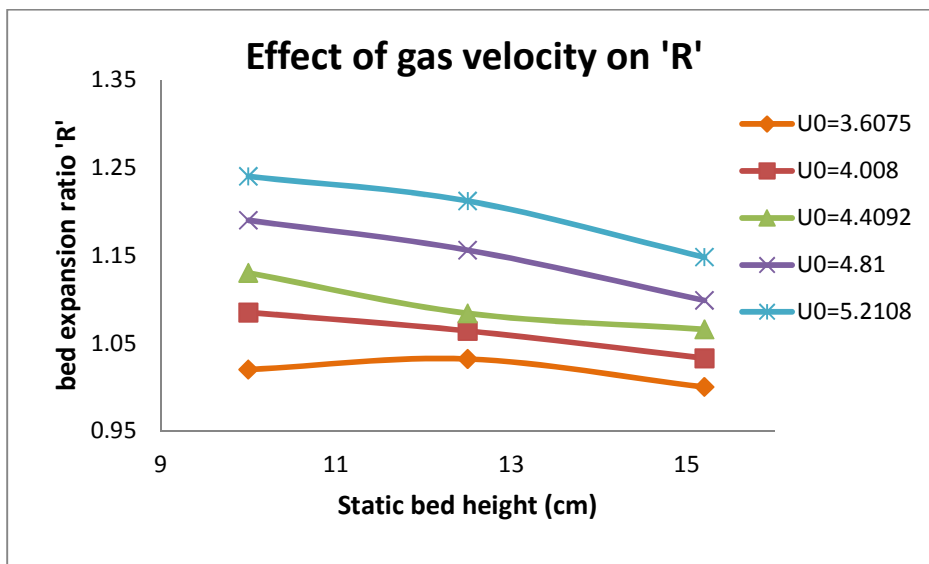


Fig 5.11. Variation of bed expansion ratio with static bed height for varying superficial gas velocity of const. mixture 40:30:30 and for cone angle of 4.61° .

(4) EFFECT OF TAPERED ANGLE (α):

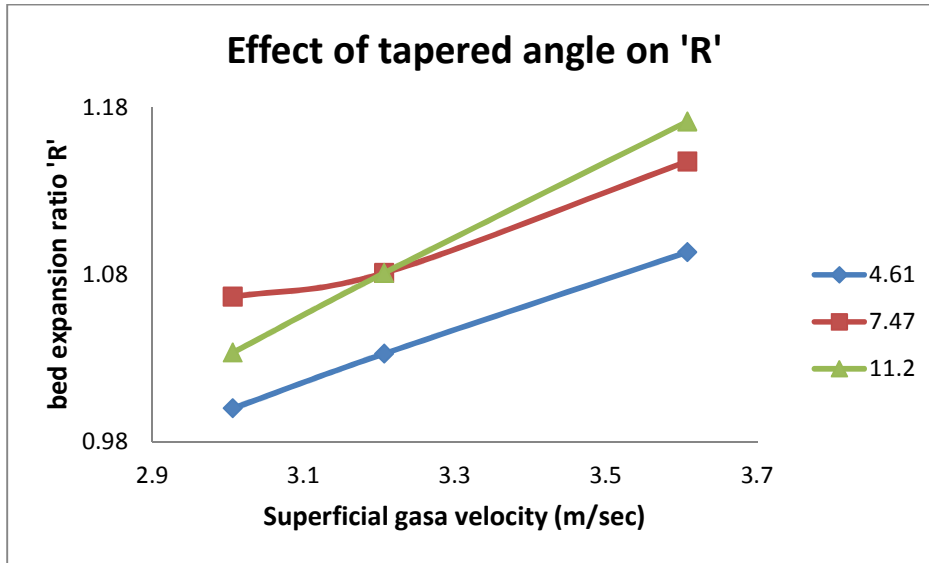


Fig 5.12. Variation of bed expansion ratio with gas superficial velocity for varying cone angles of const. $H_s=10.5$ cm and for a mixture of 20:60:20.

Discussion:

From the above figures, here also observed same as in the case of fluctuation ratio, effect of parameters i.e average particle diameter, gas velocity and tapered angle increases, bed expansion ratio is also increases. But in the case of static bed height, as increases the bed height bed expansion ratio decreases.

5.4. DEVELOPMENT OF CORRELATIONS FOR BED FLUCTUATION RATIO BY DIMENSIONAL ANALYSIS (DA):

The bed fluctuation ratio is found to depend on four dimensionless factors i.e. static bed height, average particle diameter, superficial gas velocity and tapered angle, the exponential power of those constant is obtained from dimensional analysis

$$r = K \left(\frac{G_m - G_{mf}}{G_{mf}} \right)^a \left(\frac{D_o}{D_{psm}} \right)^b \left(\frac{H_s}{D_o} \right)^c \tan(\alpha)^d$$

Development of correlation Coefficients of r by DA:

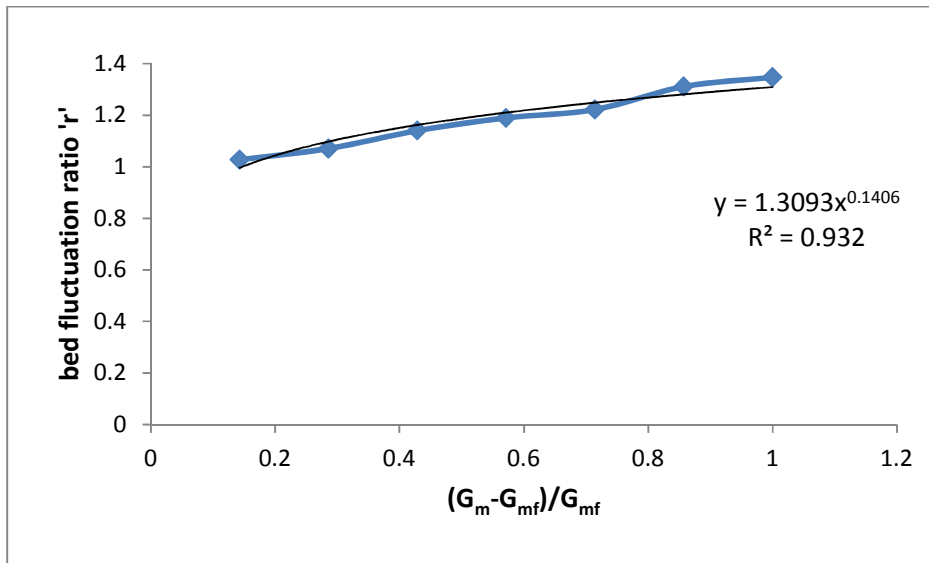


Fig 5.13. Plot of r vs $(G_m - G_{mf})/G_{mf}$.

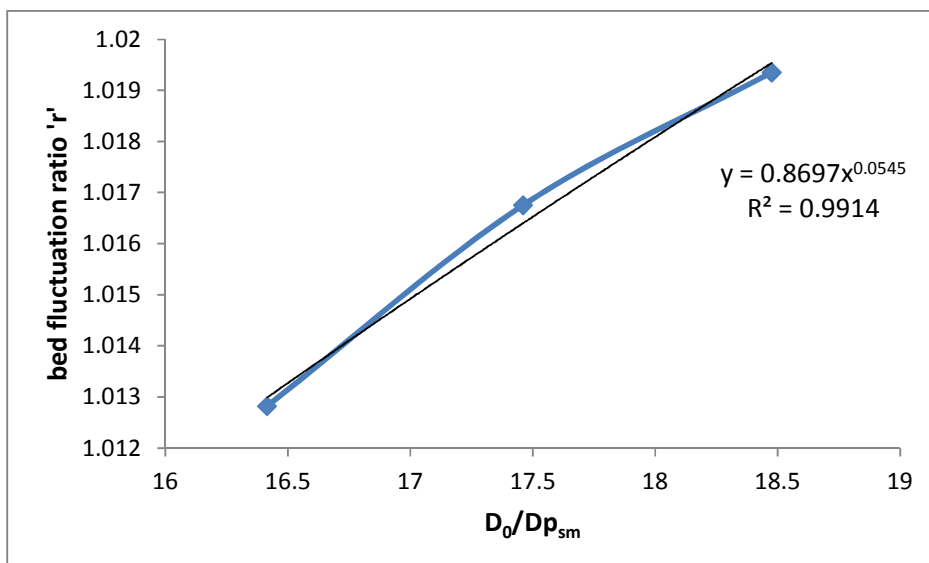


Fig 5.14. Plot of r vs D_o/D_{psm} .

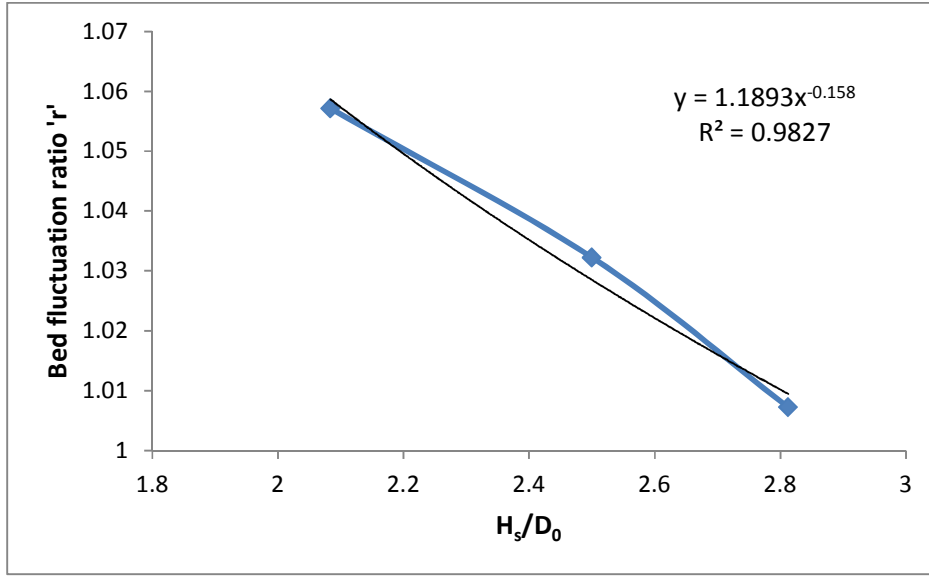


Fig 5.15. Plot of r vs. H_s/D_0 .

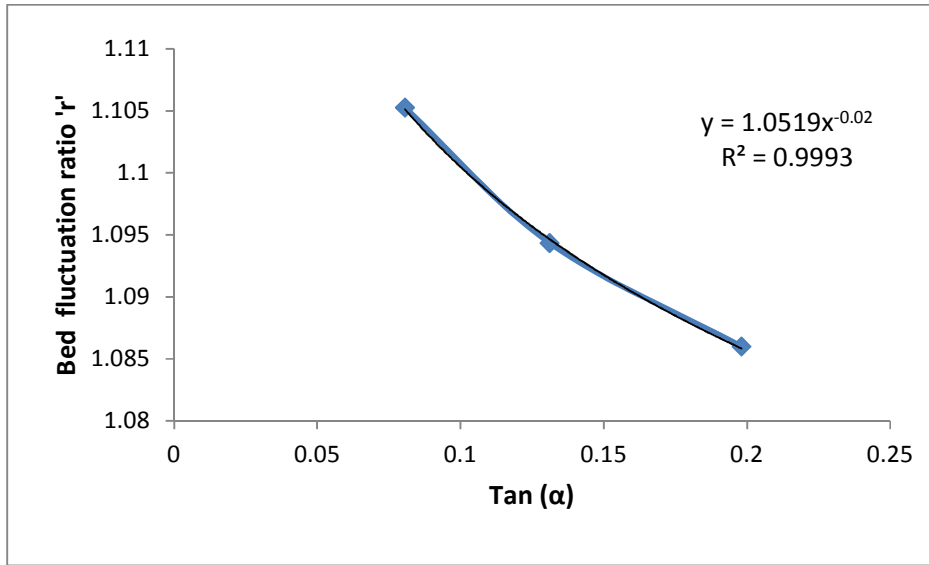


Fig 5.16. Plot of r Vs $\tan \alpha$.

From the above graphs we obtain the values $a=0.1406$; $b=0.0545$; $c=-0.158$; and $d=-0.02$

$$\text{Hence, } product = \left(\frac{G_m - G_{mf}}{G_{mf}} \right)^{0.1406} \left(\frac{D_o}{D_{psm}} \right)^{0.0545} \left(\frac{H_s}{D_o} \right)^{-0.158} \tan(\alpha)^{-0.02}$$

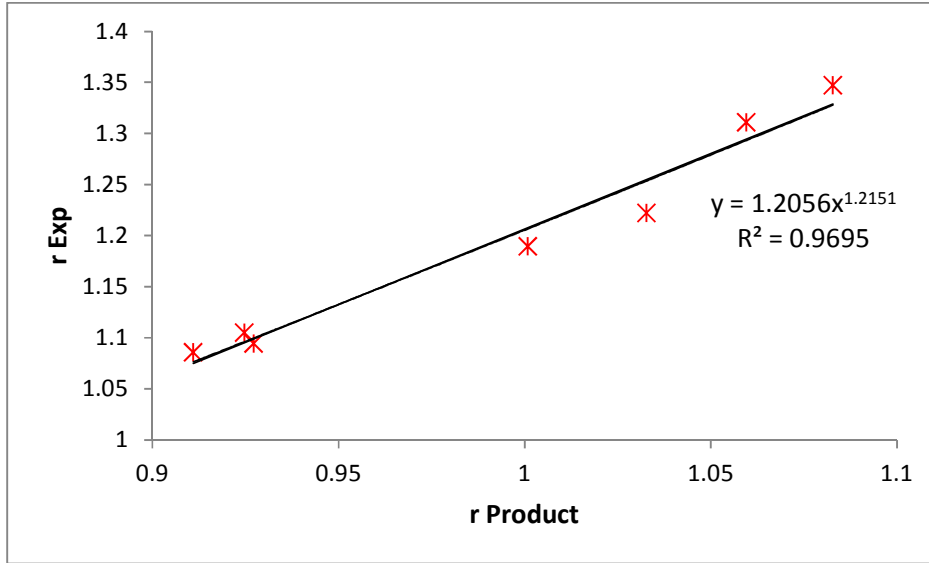


Fig 5.17. Plot of r vs. r product.

From the above graph $K=1.2056$; $n=1.2151$;

Hence the final correlation is,

$$r = 1.2056 \left(\frac{G_m - G_{mf}}{G_{mf}} \right)^{0.1708} \left(\frac{D_o}{D_{psm}} \right)^{0.0662} \left(\frac{H_s}{D_o} \right)^{-0.192} \tan(\alpha)^{-0.0243}$$

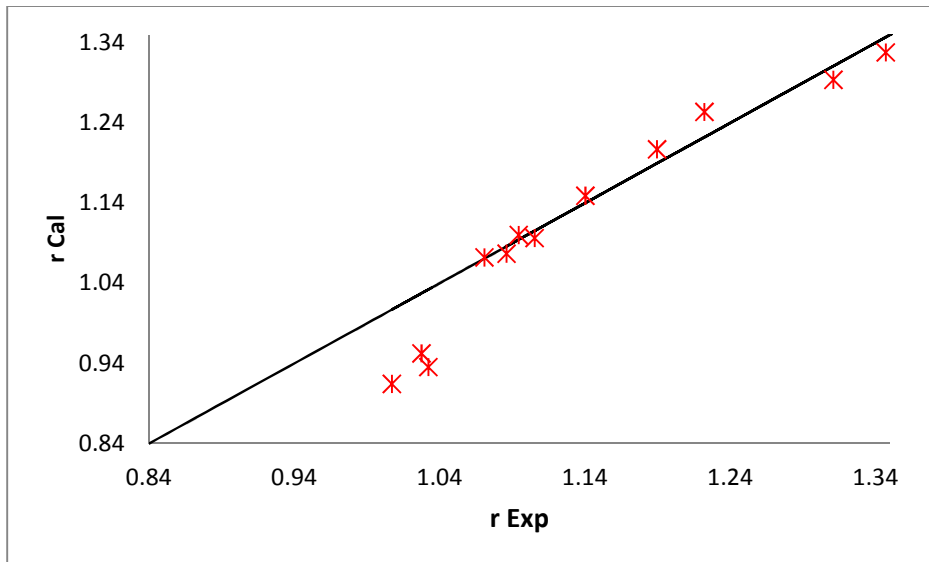


Fig 5.18. Plot of r cal vs. r exp.

5.5. DEVELOPMENT OF CORRELATIONS FOR BED EXPANSION RATIO BY DIMENSIONAL ANALYSIS (DA):

The bed expansion ratio is also found to depend on four dimensionless factors i.e. static bed height, average particle diameter, superficial gas velocity and tapered angle, the exponential power of those constant is obtained from dimensional analysis

$$R = K \left(\frac{G_m - G_{mf}}{G_{mf}} \right)^a \left(\frac{D_o}{D_{psm}} \right)^b \left(\frac{H_s}{D_o} \right)^c \tan(\alpha)^d$$

Development of correlation Coefficients of R by DA:

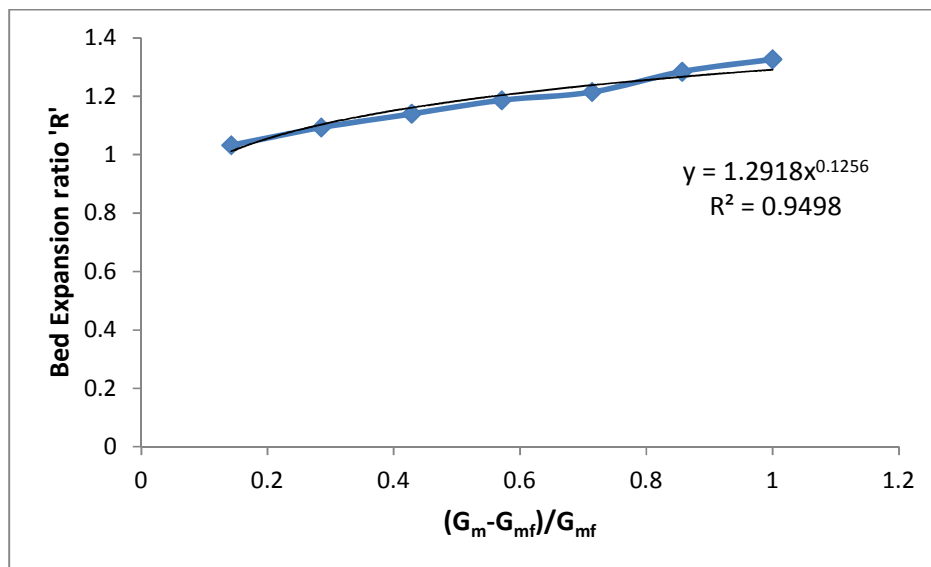


Fig 5.19. Plot of R vs $(G_m - G_{mf})/G_{mf}$.

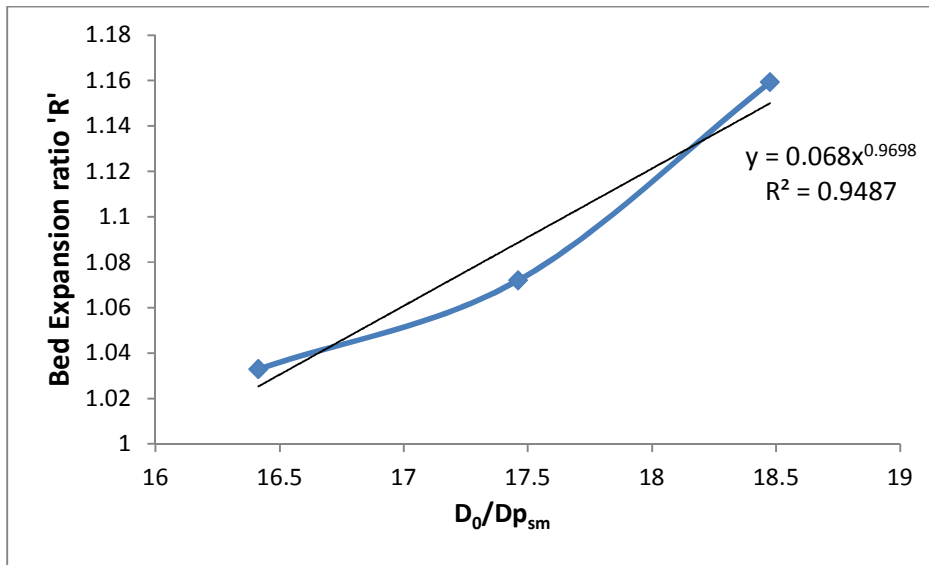


Fig 5.20. Plot of R vs $D_0/D_{p_{sm}}$.

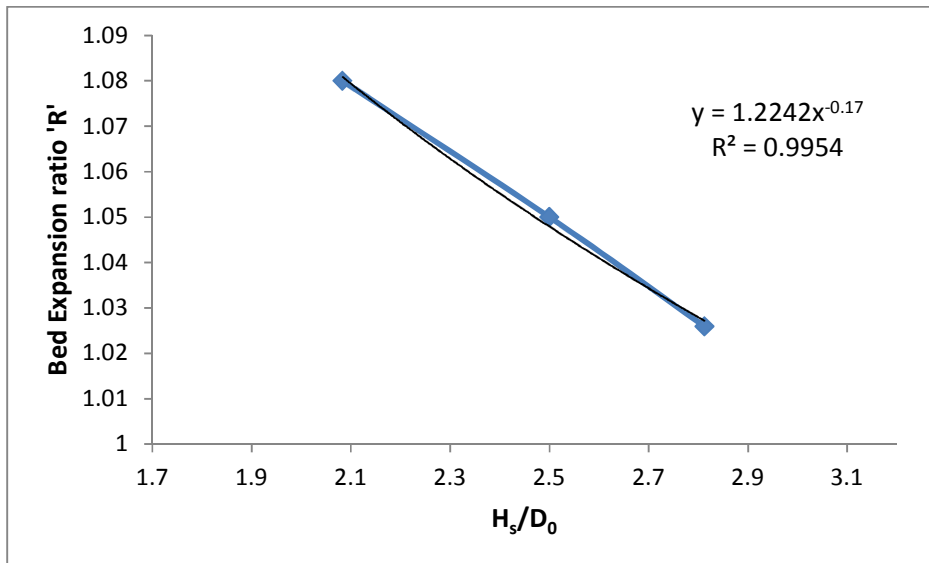


Fig 5.21. Plot of R vs. H_s/D_0 .

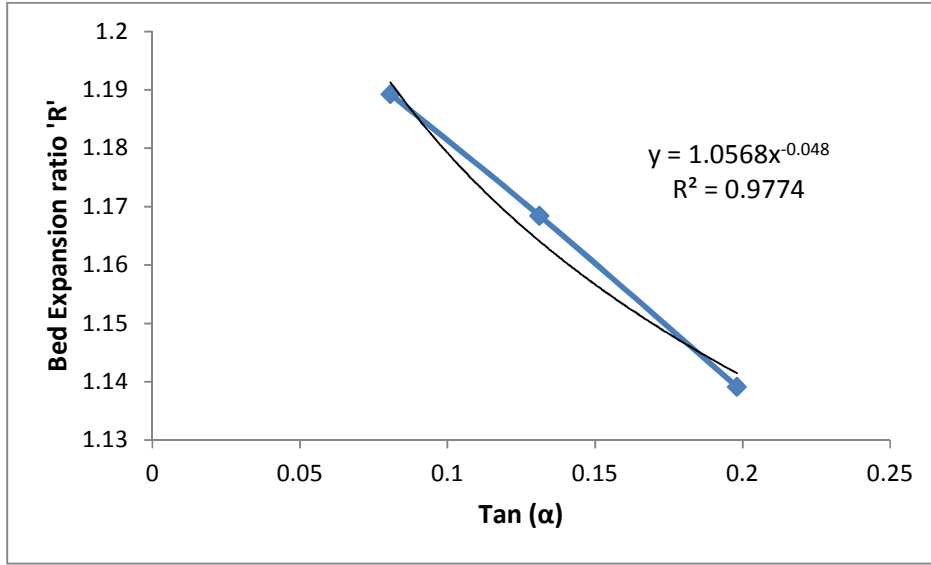


Fig 5.22. Plot of R Vs tan α.

From the above graphs we obtain the values $a=0.1256$; $b=0.9698$; $c=-0.17$; and $d=-0.048$

$$\text{Hence, } product = \left(\frac{G_m - G_{mf}}{G_{mf}} \right)^{0.1256} \left(\frac{D_o}{D_{psm}} \right)^{0.9698} \left(\frac{H_s}{D_o} \right)^{-0.17} \tan(\alpha)^{-0.048}$$

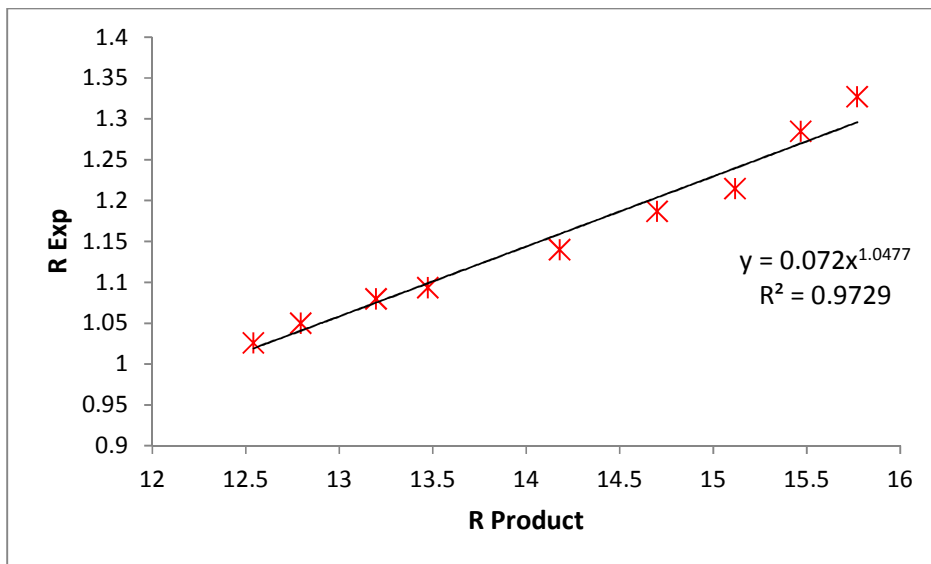


Fig 5.23. Plot of R vs. R product.

From the graph $K=0.072$; $n=1.0477$;

Hence the final correlation is,

$$R = 0.072 \left(\frac{G_m - G_{mf}}{G_{mf}} \right)^{0.1316} \left(\frac{D_o}{D_{psm}} \right)^{1.016} \left(\frac{H_s}{D_o} \right)^{-0.1781} \tan(\alpha)^{-0.0503}$$

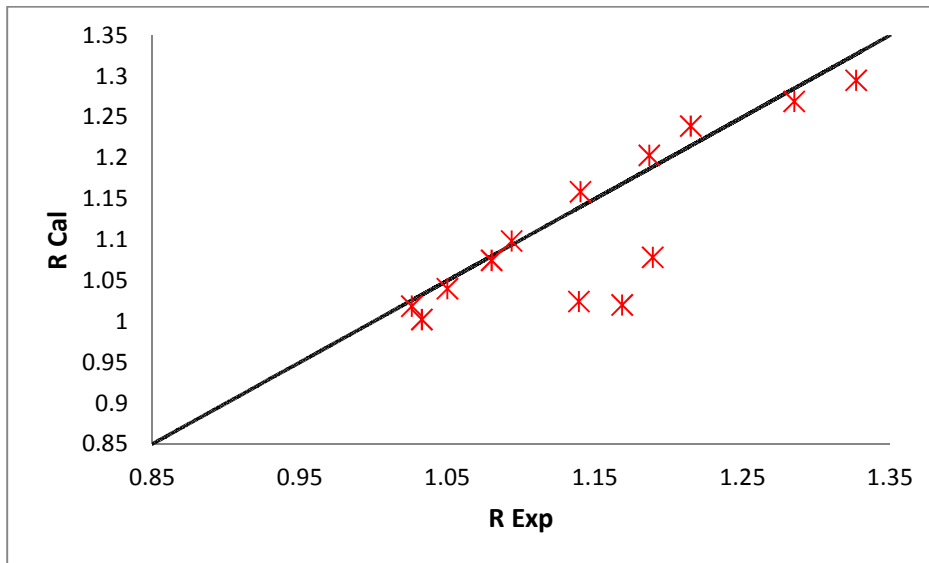


Fig 5.24. Plot of R cal vs. R exp.

From the graphs of calculated Vs experimental of fluctuation ratio and expansion ratio, it shows the points are very close to the diagonal line, except very few points. It means that the points lie on the diagonal line says that the experimental and calculated values are same. From the data of calculated and experimental values of r and R , standard deviation and mean deviations are measured and are shown in below table

Table 5.1. Deviations of r and R .

	r	R
Standard deviation	19.06	8.07
Mean deviation	7.26	6.31

5.6. DEVELOPMENT OF CORRELATIONS OF 'r' AND 'R' BY ARTIFICIAL NEURAL NETWORK (ANN) APPROACH:

From the experimental data consists 416 datasets with 5 samples, and trained with ANN network. The output data is taken from the values obtained by DA approach. The trained network mean square error for r and R are shown in fig 5.25 and fig 5.26 and It is observed that the mean square error values obtained for 1000 numbers of epochs. With the trained network simulated with the same data and obtained results. The correlations for obtained from r and R by ANN approach are

$$r = 1.20984 \left(\frac{G_m - G_{mf}}{G_{mf}} \right)^{0.1707} \left(\frac{D_o}{D_{psm}} \right)^{0.07078} \left(\frac{H_s}{D_o} \right)^{-0.1898} \tan(\alpha)^{-0.02256}$$

$$R = 0.07159 \left(\frac{G_m - G_{mf}}{G_{mf}} \right)^{0.1243} \left(\frac{D_o}{D_{psm}} \right)^{1.0154} \left(\frac{H_s}{D_o} \right)^{-0.18034} \tan(\alpha)^{-0.0504}$$

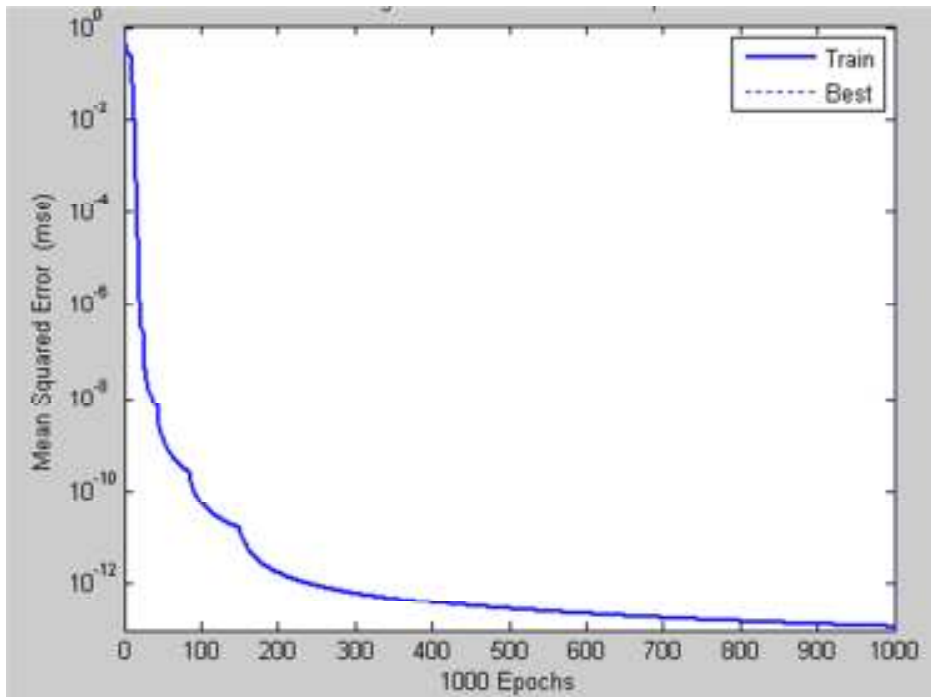


Fig 5.25. Performance plot for r.

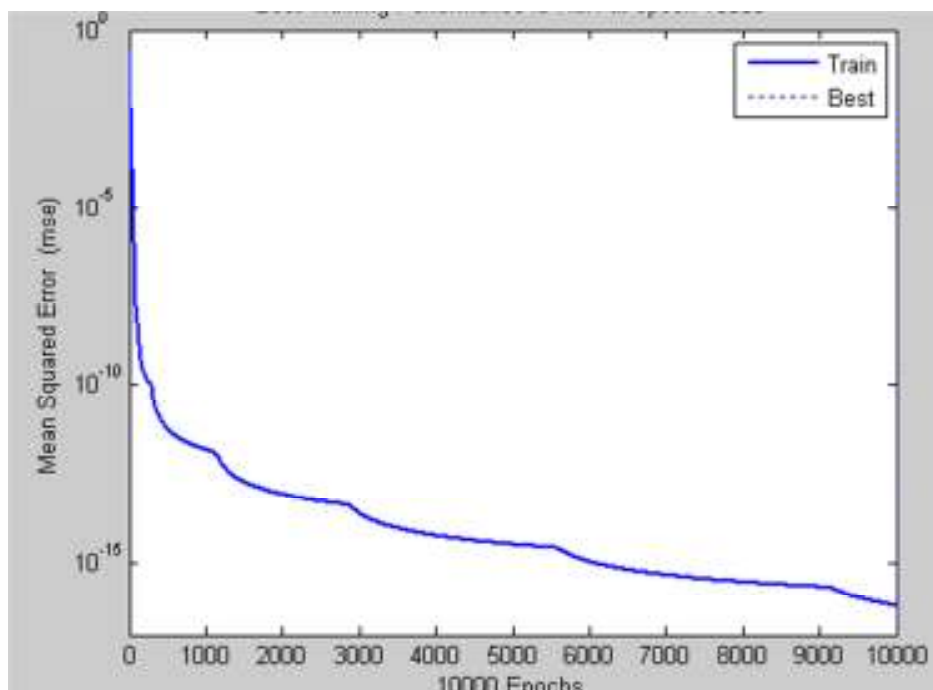


Fig 5.26. Performance plot for R.

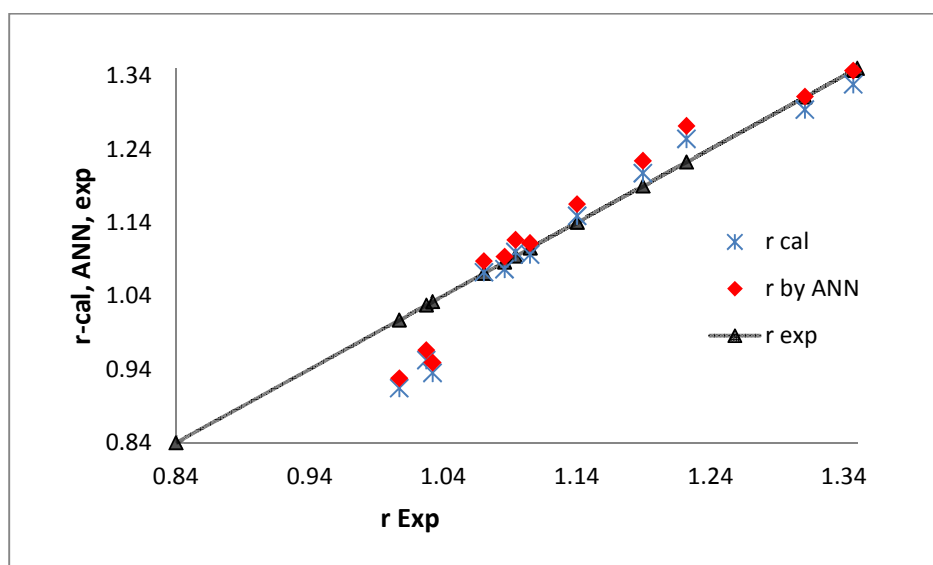


Fig 5.27. Comparison of experimental and calculated values of r by both DA and ANN approaches.

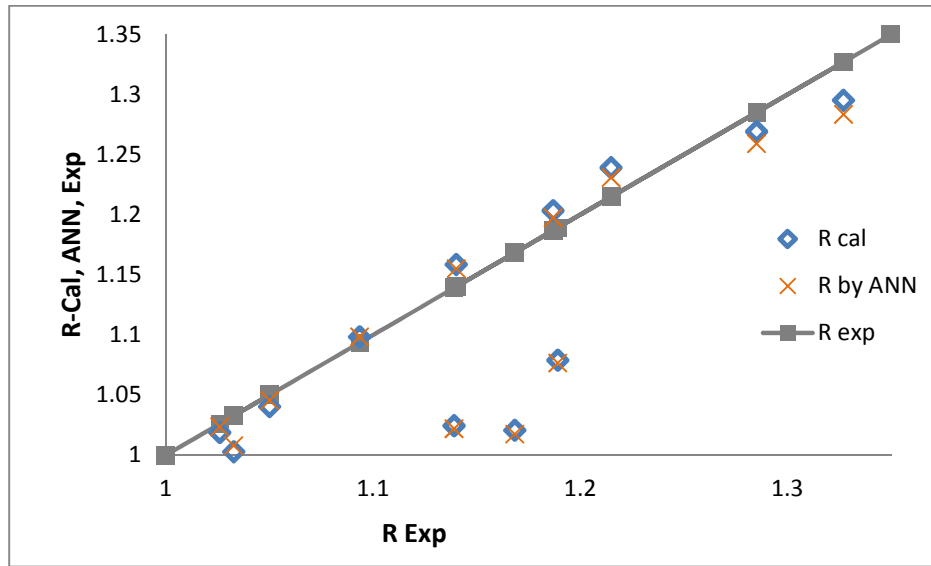


Fig 5.28. Comparison of experimental and calculated values of r by both DA and ANN approaches.

Experimental values of r and R are compare with the calculated values of r and R by both DA and ANN approaches, and deviations are found to be as shown in table 5.2

Table 5.2. Deviations of r and R by experimental with calculated values of r and R by DA and ANN approaches.

Approach	Fluctuation ratio ' r '		Expansion ratio ' R '	
	DA	ANN	DA	ANN
Standard deviation	19.06	19.31	8.07	7.92
Mean deviation	7.26	7.35	6.31	6.19

Chapter 6

Conclusion

Conclusion:

In this work, the hydrodynamic characteristics of tapered bed of ternary mixtures are studied. The experiments were carried out to interpreting the ternary mixture of glass beads with different sizes (sieve sizes of -4+5, -6+7 and -7+8) revealed that with the increase in static bed height, gas velocity, tapered angle and average particle diameter, hydrodynamic characteristics like; bed fluctuation ratio (r) and bed expansion ratio (R) decreases for static bed height and average particle diameter, increases for gas velocity and tapered angle. An ANN approach has been used to develop correlations with system parameters as static bed height, average particle dia, gas velocity and tapered angle. ANN has exhibited good performance in comparison with the dimensionless analysis. The Experimental values of bed fluctuation and expansion ratio are compared with the values calculated by DA and ANN approach. The obtained results are well within the reasonable limits, it says that ANN can be applied for various process conditions also.

References:

1. D.C. Sau, S. Mohanty, K.C. Biswal, Correlations for critical fluidization velocity and maximum bed pressure drop for heterogeneous binary mixture of irregular particles in gas–solid tapered fluidized beds, *Chemical Engineering and Processing*, 47 (2008) 2386–2390.
2. D.C. Sau, S. Mohanty, K.C. Biswal, Critical fluidization velocities and maximum bed pressure drops of homogeneous binary mixture of irregular particles in gas–solid tapered fluidized beds, *Powder Technology*, 186 (2008) 241–246.
3. K.C. Biswal, S. Sahu, G.K. Roy, Prediction of Fluctuation Ratio For Gas-Solid Fluidization of Regular Particles in Conical Vessels, *The Chemical Engineering Journal*, UK, vol 23(1982) 97-100.
4. .D. Scott, C.W. Hancher, Use of a tapered fluidized bed as a continuous bioreactor, *Biotechnology. Bio-engineering*. 18 (1976) 1393–1403.
5. C.S. Wu, J.S. Huang, R. Ohara, Hydrodynamics of tapered anaerobic fluidized beds for metabolic gas production, *Chem. Eng. Journal*, 148 (2009) 279–289.
6. S. Jing, Q. Hu, J.Wang, Y. Jin, Fluidization of coarse particles in gas–solid conical beds, *Chemical Engineering and Processing*, 39 (2000) 379–387.
7. Y. Peng, L.T. Fan, Hydrodynamic characteristics of fluidization in Liquid–solid tapered beds, *Chemical Engineering Science*, 52 (14) (1997) 2277–2290.
8. R.K. Singh, A. Suryanarayana, G.K. Roy, Prediction of minimum velocity and minimum bed pressure drop for gas–solid fluidization in conical conduits, *Can. J. Chem. Eng.* 70 (1992) 185–189.
9. D.C. Sau, S. Mohanty, K.C. Biswal, Experimental studies and empirical models for the prediction of bed expansion in gas–solid tapered fluidized beds, *Chemical Engineering and Processing* 49 (2010) 418–424.
10. A. Kumar, G.K. Roy, Artificial Neural Network-based Prediction of Bed Expansion Ratio in Gas-solid Fluidized Beds with Disk and Blade Promoters, *institute of engineers-India chemical engineering division* 85 (2004) 12-16.
11. A. Sahoo, G.K. Roy, Artificial Neural Network Approach to Segregation Characteristic of Binary Heterogeneous Mixtures in Promoted Gas Solid Fluidized Beds, *Particulate Science and technology*, 26 (2008) 574-586.

12. Y.K. Mohanty, K.C. Biswal, G.K. Roy, B.P. Mohanty, Effect of promoters on dynamics of gas – solid fluidized bed — Statistical and ANN approaches, *China Particuology*, 5 (2007) 401-407.
13. Y.K. Mohanty, B.P. Mohanty, G.K. Roy, K.C. Biswal, Effect of promoters and secondary fluidizing medium on mixing : statistical and ANN approaches, *Asia-Pac. J. Chem. Eng.* 3 (2008) 550–559.
14. Y.K. Mohanty, B.P. Mohanty, G.K. Roy, K.C. Biswal, Effect of secondary fluidizing medium on hydrodynamics of gas – solid fluidized bed — Statistical and ANN approaches, *Chemical Engineering Journal*, 148 (2009) 41-49.
15. D.C. Sau, S. Mohanty, K.C. Biswal, Prediction of critical fluidization velocity and maximum bed pressure drop for binary mixture of regular particles in gas–solid tapered fluidized beds, *Chemical Engineering and Processing* 47 (2008) 2114–2120.
16. Olazer, M., SanJose, M.J., Aguayo, A.T., Arandes, J.M., Bilbao, J., Pressure drop in conical spouted beds, *Chemical Engineering Journal*, 51 (1993) 53–60.
17. Agarwal, S.K., Roy, G.K., Packed bed pressure drop and incipient condition in a conical bed of spherical particles: a mathematical model, *Indian Chemical Engineering*, 30(3) (1988) 40-43.
18. Ergun, S., Fluid flow through packed columns, *Chemical Engineering Progress*, 48 (1952) 89–94.
19. Biswal, K.C., Roy, G.K., Prediction of Fluctuation Ratio for Gas-Solid Fluidization of Irregular Particles in Conical Vessels, *Journal of the Institution of Engineers (India)*, 6 (1983) pt CH 2
20. Biswal, K.C., Samal, B.B., Roy, G.K., Dynamics of Gas-Solid Fluidization of regular Particles in Conical Vessels, *Journal of the Institution of Engineers (India)*, 65 (1984) Pt CH 1.
21. Singh, R.K., Roy G.K. and Suryanarayana, A., Prediction of Fluctuation Ratio for Binary Mixtures of Non-Spherical Particles in Conical Beds., *Indian Journal of Chemical Technology*, 13 (2006), 139-143.
22. Singh, R. K., Studies on certain aspects of gas-solid fluidization in non-cylindrical conduits, Ph.D. Thesis, Sambalpur Univ., (India) 1997.

23. Singh, R. K. and Roy, G. K., Prediction of bed fluctuation ratio for gas-solid fluidization in cylindrical and non-cylindrical beds, Proc. Indian Chem. Cong., (2000) TP67.
24. K.C. Biswal, T.Bhowmik and G.K.Roy, Prediction of pressure drop for a conical fixed bed of spherical particles in gas-solid systems, Journal of Chemical Engg.,29 (1984) 47-50.

Appendix

Experimental Data:

Table A.1: Variation of pressure drop with superficial gas velocity for 40:30:30 mixture with $h_s=10\text{cm}$ and $\alpha=4.61^0$.

Flow rate (m ³ /hr)	Gas velocity (m/sec)	h_{\max} (cm)	h_{\min} (cm)	ΔP (cm)	ΔP (N/m ²)	r	R
12	2.4050	10	10	14	2175.4656	1	1
14	2.8058	10	10	16	2486.2464	1	1
16	3.2067	10	10	17.6	2734.8710	1	1
18	3.6075	10.3	10.1	17.2	2672.7148	1.0198	1.02
20	4.0083	11.1	10.6	19	2952.4176	1.0472	1.085
22	4.4092	11.7	10.9	20	3107.808	1.0734	1.13
24	4.8100	12.8	11	22	3418.5888	1.1636	1.19
26	5.2108	13.8	11	22.6	3511.823	1.2545	1.24

Table A.2: Variation of pressure drop with superficial gas velocity for 40:30:30 mixture with $h_s=12.5\text{cm}$ and $\alpha=4.61^0$.

Flow rate (m ³ /hr)	Gas velocity (m/sec)	h_{\max} (cm)	h_{\min} (cm)	ΔP (cm)	ΔP (N/m ²)	r	R
12	2.4050	12.5	12.5	15	2330.856	1	1
14	2.8058	12.5	12.5	18	2797.0272	1	1
16	3.2067	12.5	12.5	21	3263.1984	1	1
18	3.6075	13	12.8	19.8	3076.7299	1.0156	1.032
20	4.0083	13.5	13.1	20	3107.808	1.0305	1.064
22	4.4092	13.9	13.2	21	3263.1984	1.0530	1.084
24	4.8100	15.1	13.8	22.2	3449.6669	1.0942	1.156
26	5.2108	16.2	14.1	23.6	3667.2134	1.1489	1.212

Table A.3: Variation of pressure drop with superficial gas velocity for 40:30:30 mixture with $h_s=15.2\text{cm}$ and $\alpha=4.61^0$.

Flow rate (m^3/hr)	Gas velocity (m/sec)	h_{\max} (cm)	h_{\min} (cm)	ΔP (cm)	ΔP (N/m^2)	r	R
12	2.4050	15.2	15.2	16.4	2548.4026	1	1
14	2.8058	15.2	15.2	19.4	3014.5738	1	1
16	3.2067	15.2	15.2	23	3573.9792	1	1
18	3.6075	15.2	15.2	27	4195.5408	1	1
20	4.0083	15.8	15.6	25.4	3946.9162	1.0128	1.0329
22	4.4092	16.5	15.9	24.4	3791.5258	1.0377	1.0658
24	4.8100	17.3	16.1	24	3729.3696	1.0745	1.0987
26	5.2108	18.3	16.6	26	4040.1504	1.1024	1.148

Table A.4.: Variation of pressure drop with superficial gas velocity for 33.3:33.3:33.3 mixture with $h_s=8.5\text{cm}$ and $\alpha=4.61^0$.

Flow rate (m^3/hr)	Gas velocity (m/sec)	h_{\max} (cm)	h_{\min} (cm)	ΔP (cm)	ΔP (N/m^2)	r	R
12	2.4050	8.5	8.5	9.9	1538.365	1	1
14	2.8058	8.7	8.6	8.8	1367.4355	1.0116	1.0176
16	3.2067	9	8.7	9.2	1429.5917	1.0345	1.0412
18	3.6075	10.2	9.1	9.4	1460.6698	1.1209	1.1353
20	4.0083	11	9.2	10.6	1647.1382	1.1957	1.1882
22	4.4092	11.5	9.4	10.8	1678.2163	1.2234	1.2294
24	4.8100	12.3	9.7	12	1864.6848	1.2680	1.2941
26	5.2108	15	9.8	13.4	2082.2314	1.5306	1.4588

Table A.5.: Variation of pressure drop with superficial gas velocity for 33.3:33.3:33.3 mixture with $h_s=10.3\text{cm}$ and $\alpha=4.61^0$.

Flow rate (m^3/hr)	Gas velocity (m/sec)	h_{\max} (cm)	h_{\min} (cm)	ΔP (cm)	ΔP (N/m^2)	r	R
12	2.4050	10.3	10.3	10.6	1647.1382	1	1
14	2.8058	10.3	10.3	12	1864.6848	1	1
16	3.2067	10.6	10.4	11	1709.2944	1.0192	1.0194
18	3.6075	11.6	10.8	11.4	1771.4506	1.0741	1.0874
20	4.0083	12.8	11.2	11.6	1802.5286	1.1429	1.1650
22	4.4092	13.5	11.4	12	1864.6848	1.1842	1.2087
24	4.8100	14.1	11.5	12.4	1926.841	1.2261	1.2427
26	5.2108	15.5	11.7	13.6	2113.3094	1.3248	1.3204

Table A.6.: Variation of pressure drop with superficial gas velocity for 33.3:33.3:33.3 mixture with $h_s=12\text{cm}$ and $\alpha=4.61^0$.

Flow rate (m^3/hr)	Gas velocity (m/sec)	h_{\max} (cm)	h_{\min} (cm)	ΔP (cm)	ΔP (N/m^2)	r	R
12	2.4050	12	12	10.8	1678.21632	1	1
14	2.8058	12	12	13.2	2051.1533	1	1
16	3.2067	12.2	12.1	13.8	2144.3875	1.0083	1.0125
18	3.6075	12.8	12.4	14	2175.4656	1.0323	1.0500
20	4.0083	13.4	12.8	14.4	2237.6218	1.0469	1.0917
22	4.4092	14.7	13.3	15.2	2361.9341	1.1053	1.1667
24	4.8100	15.6	13.5	15.8	2455.1683	1.1556	1.2125
26	5.2108	16.9	13.8	16.6	2579.4806	1.2246	1.2792

Table A.7.: Variation of pressure drop with superficial gas velocity for 33.3:33.3:33.3 mixture with $h_s=13.8\text{cm}$ and $\alpha=4.61^0$.

Flow rate (m^3/hr)	Gas velocity (m/sec)	h_{\max} (cm)	h_{\min} (cm)	ΔP (cm)	ΔP (N/m^2)	r	R
12	2.4050	13.8	13.8	12	1864.6848	1	1
14	2.8058	13.8	13.8	14.9	2315.317	1	1
16	3.2067	13.8	13.8	17.3	2688.2539	1	1
18	3.6075	14	13.9	15.7	2439.6293	1.0072	1.0109
20	4.0083	14.9	14.6	15.5	2408.5512	1.0205	1.0688
22	4.4092	15.5	14.8	15.8	2455.1683	1.0473	1.0978
24	4.8100	16.3	15.1	16.6	2579.4806	1.0795	1.1377
26	5.2108	17.6	15.8	17	2641.6368	1.1139	1.2101

Table A.8.: Variation of pressure drop with superficial gas velocity for 20:60:20 mixture with $h_s=10.7\text{cm}$ and $\alpha=4.61^0$.

Flow rate (m^3/hr)	Gas velocity (m/sec)	h_{\max} (cm)	h_{\min} (cm)	ΔP (cm)	ΔP (N/m^2)	r	R
12	2.4050	10.7	10.7	11.7	1818.0677	1	1
14	2.8058	10.7	10.7	14.3	2222.0827	1	1
16	3.2067	11.2	10.9	12.5	1942.38	1.0275	1.0327
18	3.6075	12.1	11.3	12.7	1973.4581	1.0708	1.0935
20	4.0083	13	11.4	13	2020.0752	1.1404	1.1402
22	4.4092	13.8	11.6	13.6	2113.3094	1.1897	1.1869
24	4.8100	14.3	11.7	13.9	2159.9266	1.2222	1.2150
26	5.2108	15.6	11.9	15	2330.856	1.3109	1.2850
28	5.6117	16.3	12.1	15.9	2470.7074	1.3471	1.3271

Table A.9.: Variation of pressure drop with superficial gas velocity for 20:60:20 mixture with $h_s=12.2\text{cm}$ and $\alpha=4.61^0$.

Flow rate (m^3/hr)	Gas velocity (m/sec)	h_{\max} (cm)	h_{\min} (cm)	ΔP (cm)	ΔP (N/m^2)	r	R
12	2.4050	12.2	12.2	11.1	1724.8334	1	1
14	2.8058	12.2	12.2	14	2175.4656	1	1
16	3.2067	12.2	12.2	16.1	2501.7854	1	1
18	3.6075	12.6	12.4	13.9	2159.9266	1.0161	1.0246
20	4.0083	13.5	13	15	2330.856	1.0385	1.0861
22	4.4092	14.4	13.2	14.7	2284.2389	1.0909	1.1311
24	4.8100	15.2	13.3	15.7	2439.6293	1.1429	1.1680
26	5.2108	15.9	13.4	16.7	2595.0197	1.1866	1.2008
28	5.6117	17.1	13.6	17.6	2734.871	1.2574	1.2582

Table A.10: Variation of pressure drop with superficial gas velocity for 20:60:20 mixture with $h_s=14.7\text{cm}$ and $\alpha=4.61^0$.

Flow rate (m^3/hr)	Gas velocity (m/sec)	h_{\max} (cm)	h_{\min} (cm)	ΔP (cm)	ΔP (N/m^2)	r	R
12	2.4050	14.7	14.7	12.1	1880.2238	1	1
14	2.8058	14.7	14.7	14.2	2206.5437	1	1
16	3.2067	14.7	14.7	18.9	2936.8786	1	1
18	3.6075	14.7	14.7	20.3	3154.4251	1	1
20	4.0083	14.9	14.8	17.6	2734.871	1.0068	1.0102
22	4.4092	16.6	15.8	17	2641.6368	1.0506	1.1020
24	4.8100	17	16	17.2	2672.7149	1.0625	1.1224
26	5.2108	18.1	16.2	18	2797.0272	1.1173	1.1667
28	5.6117	18.9	16.6	19.7	3061.1909	1.1386	1.2075

Table A.11: Variation of pressure drop with superficial gas velocity for 20:20:60 mixture with $h_s=10\text{cm}$ and $\alpha=4.61^0$.

Flow rate (m^3/hr)	Gas velocity (m/sec)	h_{\max} (cm)	h_{\min} (cm)	ΔP (cm)	ΔP (N/m^2)	r	R
12	2.4050	10	10	11.8	1833.6067	1	1
14	2.8058	10	10	12.4	1926.8410	1	1
16	3.2067	11.1	10.5	12	1864.6848	1.0571	1.0800
18	3.6075	12	10.7	12.4	1926.8410	1.2617	1.2100
20	4.0083	13.5	11.1	13	2020.0752	1.3514	1.3050
22	4.4092	15	11.6	14.4	2237.6218	1.4052	1.3950
24	4.8100	16.3	11.5	15	2330.8560	1.4696	1.4200
26	5.2108	16.9	11.8	15.2	2361.9341	1.4322	1.4350

Table A.12: Variation of pressure drop with superficial gas velocity for 20:20:60 mixture with $h_s=12\text{cm}$ and $\alpha=4.61^0$.

Flow rate (m^3/hr)	Gas velocity (m/sec)	h_{\max} (cm)	h_{\min} (cm)	ΔP (cm)	ΔP (N/m^2)	r	R
12	2.4050	12	12	12.2	1895.7629	1	1
14	2.8058	12	12	15.6	2424.0902	1	1
16	3.2067	12.8	12.4	14	2175.4656	1.0323	1.0500
18	3.6075	13.4	12.8	14.8	2299.7779	1.0469	1.0917
20	4.0083	14.3	12.9	15.2	2361.9341	1.1085	1.1333
22	4.4092	15.1	13.1	15.6	2424.0902	1.1527	1.1750
24	4.8100	16.5	13.5	16.4	2548.4026	1.2222	1.2500
26	5.2108	17.7	13.4	17.6	2734.8710	1.3209	1.2958

Table A.13: Variation of pressure drop with superficial gas velocity for 20:20:60 mixture with $h_s=103.5\text{cm}$ and $\alpha=4.61^0$.

Flow rate (m^3/hr)	Gas velocity (m/sec)	h_{\max} (cm)	h_{\min} (cm)	ΔP (cm)	ΔP (N/m^2)	r	R
12	2.4050	13.5	13.5	15.4	2393.0122	1	1
14	2.8058	13.5	13.5	18.4	2859.1834	1	1
16	3.2067	13.9	13.8	16.4	2548.4026	1.0072	1.0259
18	3.6075	14.5	13.9	16.8	2610.5587	1.0432	1.0519
20	4.0083	14.8	14.4	17.2	2672.7149	1.0278	1.0815
22	4.4092	16.4	14.9	18.4	2859.1834	1.1007	1.1593
24	4.8100	17.7	15	19.4	3014.5738	1.1800	1.2111
26	5.2108	18.3	15.2	20	3107.8080	1.2039	1.2407

Table A.14: Variation of pressure drop with superficial gas velocity for 20:20:60 mixture with $h_s=15\text{cm}$ and $\alpha=4.61^0$.

Flow rate (m^3/hr)	Gas velocity (m/sec)	h_{\max} (cm)	h_{\min} (cm)	ΔP (cm)	ΔP (N/m^2)	r	R
12	2.4050	15	15	17.4	2703.7930	1	1
14	2.8058	15	15	20.4	3169.9642	1	1
16	3.2067	15	15	23.4	3636.1354	1	1
18	3.6075	15.8	15.5	17.2	2672.7149	1.0194	1.0433
20	4.0083	15.9	15.5	16.9	2626.0978	1.0258	1.0467
22	4.4092	16.9	15.9	16.7	2595.0197	1.0629	1.0933
24	4.8100	17.5	16.4	16.8	2610.5587	1.0671	1.1300
26	5.2108	18.6	16.8	18	2797.0272	1.1071	1.1800

Table A.15: variation of pressure drop with superficial gas velocity for 40:30:30 mixture with $h_s=8.5\text{cm}$ and $\alpha=7.47^0$.

Flow rate (m^3/hr)	Gas velocity (m/sec)	h_{\max} (cm)	h_{\min} (cm)	ΔP (cm)	ΔP (N/m^2)	r	R
9	1.8038	8.5	8.5	8.3	1289.7403	1	1
10	2.0042	8.5	8.5	9.3	1445.1307	1	1
11	2.2046	8.6	8.5	8.4	1305.2794	1.0118	1.0059
12	2.4050	8.8	8.6	8.2	1274.2013	1.0233	1.0235
13	2.6054	9.1	8.8	8.2	1274.2013	1.0341	1.0529
14	2.8058	9.6	9.1	8.3	1289.7403	1.0549	1.1000
15	3.0063	10.1	9.3	8.2	1274.2013	1.0860	1.1412
16	3.2067	10.5	9.5	8.2	1274.2013	1.1053	1.1765
17	3.4071	10.9	9.6	8.2	1274.2013	1.1354	1.2059
18	3.6075	11.4	9.9	8.2	1274.2013	1.1515	1.2529

Table A.16: variation of pressure drop with superficial gas velocity for 40:30:30 mixture with $h_s=9.5\text{cm}$ and $\alpha=7.47^0$.

Flow rate (m^3/hr)	Gas velocity (m/sec)	h_{\max} (cm)	h_{\min} (cm)	ΔP (cm)	ΔP (N/m^2)	r	R
9	1.8038	9.5	9.5	8.2	1274.2013	1	1
10	2.0042	9.5	9.5	9	1398.5136	1	1
11	2.2046	9.5	9.5	10.5	1631.5992	1	1
12	2.4050	9.6	9.5	10	1553.9040	1.0105	1.0053
13	2.6054	9.8	9.6	9.8	1522.8259	1.0208	1.0211
14	2.8058	10.4	9.8	9.9	1538.3650	1.0612	1.0632
15	3.0063	10.7	10.1	9.6	1491.7478	1.0594	1.0947
16	3.2067	11.1	10.3	9.4	1460.6698	1.0777	1.1263
17	3.4071	11.5	10.5	9.5	1476.2088	1.0952	1.1579
18	3.6075	11.8	10.6	9.5	1476.2088	1.1132	1.1789

Table A.17: variation of pressure drop with superficial gas velocity for 40:30:30 mixture with $h_s=10.5\text{cm}$ and $\alpha=7.47^0$.

Flow rate (m^3/hr)	Gas velocity (m/sec)	h_{\max} (cm)	h_{\min} (cm)	ΔP (cm)	ΔP (N/m^2)	r	R
9	1.8038	10.5	10.5	9.2	1429.5917	1	1
10	2.0042	10.5	10.5	10.1	1569.4430	1	1
11	2.2046	10.5	10.5	12.1	1880.2238	1	1
12	2.4050	10.6	10.5	11.1	1724.8334	1.0095	1.0048
13	2.6054	10.7	10.6	10.9	1693.7554	1.0094	1.0143
14	2.8058	11	10.8	10.9	1693.7554	1.0185	1.0381
15	3.0063	11.3	10.9	10.8	1678.2163	1.0367	1.0571
16	3.2067	11.7	11.2	10.8	1678.2163	1.0446	1.0905
17	3.4071	12.2	11.6	10.8	1678.2163	1.0517	1.1333
18	3.6075	12.5	11.8	10.8	1678.2163	1.0593	1.1571

Table A.18: Variation of pressure drop with superficial gas velocity for 40:30:30 mixture with $h_s=11.5\text{cm}$ and $\alpha=7.47^0$.

Flow rate (m^3/hr)	Gas velocity (m/sec)	h_{\max} (cm)	h_{\min} (cm)	ΔP (cm)	ΔP (N/m^2)	r	R
9	1.8038	11.5	11.5	9.1	1414.0526	1	1
10	2.0042	11.5	11.5	10.3	1600.5211	1	1
11	2.2046	11.5	11.5	11.1	1724.8334	1	1
12	2.4050	11.5	11.5	14.1	2191.0046	1	1
13	2.6054	11.5	11.5	14.6	2268.6998	1	1
14	2.8058	11.7	11.6	13.6	2113.3094	1.0086	1.0130
15	3.0063	12.2	11.8	12.8	1988.9971	1.0339	1.0435
16	3.2067	12.5	12	13.1	2035.6142	1.0417	1.0652
17	3.4071	12.8	12	12.8	1988.9971	1.0667	1.0783
18	3.6075	13.3	12.5	12.8	1988.9971	1.0640	1.1217

Table A.19: variation of pressure drop with superficial gas velocity for 33.3:33.3:33.3 mixture with $h_s=8.5\text{cm}$ and $\alpha=7.47^0$.

Flow rate (m^3/hr)	Gas velocity (m/sec)	h_{\max} (cm)	h_{\min} (cm)	ΔP (cm)	ΔP (N/m^2)	r	R
9	1.8038	8.5	8.5	8.5	1320.8184	1	1
10	2.0042	8.5	8.5	9.4	1460.6698	1	1
11	2.2046	8.6	8.5	8.9	1382.9746	1.0118	1.0059
12	2.4050	8.8	8.6	8.7	1351.8965	1.0233	1.0235
13	2.6054	9.3	8.9	8.7	1351.8965	1.0449	1.0706
14	2.8058	9.8	9.2	8.7	1351.8965	1.0652	1.1176
15	3.0063	10.2	9.4	8.7	1351.8965	1.0851	1.1529
16	3.2067	10.7	9.6	8.7	1351.8965	1.1146	1.1941
17	3.4071	11	9.7	8.7	1351.8965	1.1340	1.2176
18	3.6075	11.5	10	8.7	1351.8965	1.1500	1.2647

Table A.20: variation of pressure drop with superficial gas velocity for 33.3:33.3:33.3 mixture with $h_s=9.5\text{cm}$ and $\alpha=7.47^0$.

Flow rate (m^3/hr)	Gas velocity (m/sec)	h_{\max} (cm)	h_{\min} (cm)	ΔP (cm)	ΔP (N/m^2)	r	R
9	1.8038	9.5	9.5	8.5	1320.8184	1	1
10	2.0042	9.5	9.5	9.3	1445.1307	1	1
11	2.2046	9.5	9.5	11.1	1724.8334	1	1
12	2.4050	9.6	9.5	9.8	1522.8259	1.0105	1.0053
13	2.6054	9.8	9.6	9.6	1491.7478	1.0208	1.0211
14	2.8058	10.1	9.8	9.4	1460.6698	1.0306	1.0474
15	3.0063	10.7	10	9.4	1460.6698	1.0700	1.0895
16	3.2067	11.1	10.3	9.4	1460.6698	1.0777	1.1263
17	3.4071	11.3	10.5	9.4	1460.6698	1.0762	1.1474
18	3.6075	11.8	10.7	9.4	1460.6698	1.1028	1.1842

Table A.21: variation of pressure drop with superficial gas velocity for 33.3:33.3:33.3 mixture with $h_s=10.5\text{cm}$ and $\alpha=7.47^0$.

Flow rate (m^3/hr)	Gas velocity (m/sec)	h_{\max} (cm)	h_{\min} (cm)	ΔP (cm)	ΔP (N/m^2)	r	R
9	1.8038	10.5	10.5	8.5	1320.8184	1	1
10	2.0042	10.5	10.5	9.6	1491.7478	1	1
11	2.2046	10.5	10.5	11	1709.2944	1	1
12	2.4050	10.5	10.5	13.4	2082.2314	1	1
13	2.6054	10.7	10.6	12.2	1895.7629	1.0094	1.0143
14	2.8058	11	10.8	11.5	1786.9896	1.0185	1.0381
15	3.0063	11.3	11	11.1	1724.8334	1.0273	1.0619
16	3.2067	11.7	11.2	10.9	1693.7554	1.0446	1.0905
17	3.4071	12	11.3	10.9	1693.7554	1.0619	1.1095
18	3.6075	12.4	11.6	10.9	1693.7554	1.0690	1.1429

Table A.22: variation of pressure drop with superficial gas velocity for 33.3:33.3:33.3 mixture with $h_s=11.5\text{cm}$ and $\alpha=7.47^0$.

Flow rate (m^3/hr)	Gas velocity (m/sec)	h_{\max} (cm)	h_{\min} (cm)	ΔP (cm)	ΔP (N/m^2)	r	R
9	1.8038	11.5	11.5	8.9	1382.9746	1	1
10	2.0042	11.5	11.5	9.7	1507.2869	1	1
11	2.2046	11.5	11.5	11.3	1755.9115	1	1
12	2.4050	11.5	11.5	13.5	2097.7704	1	1
13	2.6054	11.5	11.5	15.1	2346.3950	1	1
14	2.8058	11.7	11.6	13.7	2128.8485	1.0086	1.0130
15	3.0063	12.1	11.8	12.7	1973.4581	1.0254	1.0391
16	3.2067	12.7	12.2	12.3	1911.3019	1.0410	1.0826
17	3.4071	13	12.5	12.3	1911.3019	1.0400	1.1087
18	3.6075	13.5	12.7	12.3	1911.3019	1.0630	1.1391

Table A.23: variation of pressure drop with superficial gas velocity for 20:60:20 mixture with $h_s=8.5\text{cm}$ and $\alpha=7.47^0$.

Flow rate (m^3/hr)	Gas velocity (m/sec)	h_{\max} (cm)	h_{\min} (cm)	ΔP (cm)	ΔP (N/m^2)	r	R
9	1.8038	8.5	8.5	8.4	1305.2794	1	1
10	2.0042	8.5	8.5	9.6	1491.7478	1	1
11	2.2046	8.6	8.5	8.9	1382.9746	1.0118	1.0059
12	2.4050	8.8	8.6	8.6	1336.3574	1.0233	1.0235
13	2.6054	9.1	8.8	8.4	1305.2794	1.0341	1.0529
14	2.8058	9.7	9.1	8.4	1305.2794	1.0659	1.1059
15	3.0063	10.3	9.3	8.4	1305.2794	1.1075	1.1529
16	3.2067	10.5	9.5	8.4	1305.2794	1.1053	1.1765
17	3.4071	11	9.7	8.4	1305.2794	1.1340	1.2176
18	3.6075	11.6	9.8	8.4	1305.2794	1.1837	1.2588

Table A.24: variation of pressure drop with superficial gas velocity for 20:60:20 mixture with $h_s=9.5\text{cm}$ and $\alpha=7.47^0$.

Flow rate (m^3/hr)	Gas velocity (m/sec)	h_{\max} (cm)	h_{\min} (cm)	ΔP (cm)	ΔP (N/m^2)	r	R
9	1.8038	9.5	9.5	8.5	1320.8184	1	1
10	2.0042	9.5	9.5	9.6	1491.7478	1	1
11	2.2046	9.5	9.5	11.1	1724.8334	1	1
12	2.4050	9.6	9.5	9.8	1522.8259	1.0105	1.0053
13	2.6054	10.1	9.7	9.6	1491.7478	1.0412	1.0421
14	2.8058	10.4	10	9.6	1491.7478	1.0400	1.0737
15	3.0063	10.7	10.2	9.4	1460.6698	1.0490	1.1000
16	3.2067	11.2	10.4	9.4	1460.6698	1.0769	1.1368
17	3.4071	11.6	10.6	9.4	1460.6698	1.0943	1.1684
18	3.6075	12	10.8	9.4	1460.6698	1.1111	1.2000

Table A.25: variation of pressure drop with superficial gas velocity for 20:60:20 mixture with $h_s=10.5\text{cm}$ and $\alpha=7.47^0$.

Flow rate (m^3/hr)	Gas velocity (m/sec)	h_{\max} (cm)	h_{\min} (cm)	ΔP (cm)	ΔP (N/m^2)	r	R
9	1.8038	10.5	10.5	8.7	1351.8965	1	1
10	2.0042	10.5	10.5	9.8	1522.8259	1	1
11	2.2046	10.5	10.5	11.4	1771.4506	1	1
12	2.4050	10.5	10.5	12.9	2004.5362	1	1
13	2.6054	10.7	10.6	12	1864.6848	1.0094	1.0143
14	2.8058	11	10.8	11.1	1724.8334	1.0185	1.0381
15	3.0063	11.4	11	10.6	1647.1382	1.0364	1.0667
16	3.2067	11.6	11.1	10.4	1616.0602	1.0450	1.0810
17	3.4071	12	11.4	10.4	1616.0602	1.0526	1.1143
18	3.6075	12.5	11.6	10.4	1616.0602	1.0776	1.1476

Table A.26: variation of pressure drop with superficial gas velocity for 20:60:20 mixture with $h_s=11.5\text{cm}$ and $\alpha=7.47^0$.

Flow rate (m^3/hr)	Gas velocity (m/sec)	h_{\max} (cm)	h_{\min} (cm)	ΔP (cm)	ΔP (N/m^2)	r	R
9	1.8038	11.5	11.5	8.7	1351.8965	1	1
10	2.0042	11.5	11.5	9.7	1507.2869	1	1
11	2.2046	11.5	11.5	11.5	1786.9896	1	1
12	2.4050	11.5	11.5	13.5	2097.7704	1	1
13	2.6054	11.5	11.5	14.8	2299.7779	1	1
14	2.8058	11.7	11.6	11.9	1849.1458	1.0086	1.0130
15	3.0063	12	11.7	1.9	295.2418	1.0256	1.0304
16	3.2067	12.2	11.9	11.7	1818.0677	1.0252	1.0478
17	3.4071	12.6	12.1	11.5	1786.9896	1.0413	1.0739
18	3.6075	13.1	12.3	11.5	1786.9896	1.0650	1.1043

Table A.27: variation of pressure drop with superficial gas velocity for 20:20:60 mixture with $h_s=8.5\text{cm}$ and $\alpha=7.47^0$.

Flow rate (m^3/hr)	Gas velocity (m/sec)	h_{\max} (cm)	h_{\min} (cm)	ΔP (cm)	ΔP (N/m^2)	r	R
9	1.8038	8.5	8.5	8.5	1320.8184	1	1
10	2.0042	8.7	8.6	8.3	1289.74032	1.011627907	1.017647059
11	2.2046	8.9	8.7	8.3	1289.74032	1.022988506	1.035294118
12	2.4050	9.3	8.9	8.1	1258.66224	1.04494382	1.070588235
13	2.6054	9.7	9.1	8.1	1258.66224	1.065934066	1.105882353
14	2.8058	10.2	9.4	7.9	1227.58416	1.085106383	1.152941176
15	3.0063	10.6	9.7	7.9	1227.58416	1.092783505	1.194117647
16	3.2067	11.1	9.8	7.9	1227.58416	1.132653061	1.229411765
17	3.4071	11.4	9.9	7.9	1227.58416	1.151515152	1.252941176
18	3.6075	12	10.2	7.9	1227.58416	1.176470588	1.305882353

Table A.28: variation of pressure drop with superficial gas velocity for 20:20:60 mixture with $h_s=9.5\text{cm}$ and $\alpha=7.47^0$.

Flow rate (m^3/hr)	Gas velocity (m/sec)	h_{\max} (cm)	h_{\min} (cm)	ΔP (cm)	ΔP (N/m^2)	r	R
9	1.8038	9.5	9.5	9.4	1320.8184	1	1
10	2.0042	9.5	9.5	10.6	1289.7403	1.0116	1.0176
11	2.2046	9.6	9.5	9.6	1289.7403	1.0230	1.0353
12	2.4050	9.8	9.6	9.4	1258.6622	1.0449	1.0706
13	2.6054	10.1	9.8	9.4	1258.6622	1.0659	1.1059
14	2.8058	10.5	10	9.2	1227.5842	1.0851	1.1529
15	3.0063	10.9	10.2	9	1227.5842	1.0928	1.1941
16	3.2067	11.3	10.5	9	1227.5842	1.1327	1.2294
17	3.4071	11.6	10.7	9	1227.5842	1.1515	1.2529
18	3.6075	12.1	10.8	9	1227.5842	1.1765	1.3059

Table A.29: variation of pressure drop with superficial gas velocity for 20:20:60 mixture with $h_s=10.5\text{cm}$ and $\alpha=7.47^0$.

Flow rate (m^3/hr)	Gas velocity (m/sec)	h_{\max} (cm)	h_{\min} (cm)	ΔP (cm)	ΔP (N/m^2)	r	R
9	1.8038	10.5	10.5	9.6	1491.7478	1	1
10	2.0042	10.5	10.5	10.8	1678.2163	1	1
11	2.2046	10.5	10.5	12.7	1973.4581	1	1
12	2.4050	10.5	10.5	12.9	2004.5362	1	1
13	2.6054	10.8	10.6	10.6	1647.1382	1.0189	1.0190
14	2.8058	11.1	10.8	10.4	1616.0602	1.0278	1.0429
15	3.0063	11.4	11	10.2	1584.9821	1.0364	1.0667
16	3.2067	12	11.2	10.2	1584.9821	1.0714	1.1048
17	3.4071	12.5	11.5	10.2	1584.9821	1.0870	1.1429
18	3.6075	12.7	11.7	10.2	1584.9821	1.0855	1.1619

Table A.30: variation of pressure drop with superficial gas velocity for 20:20:60 mixture with $h_s=11.5\text{cm}$ and $\alpha=7.47^0$.

Flow rate (m^3/hr)	Gas velocity (m/sec)	h_{\max} (cm)	h_{\min} (cm)	ΔP (cm)	ΔP (N/m^2)	r	R
9	1.8038	11.5	11.5	9.9	1538.3650	1	1
10	2.0042	11.5	11.5	10.9	1693.7554	1	1
11	2.2046	11.5	11.5	12.7	1973.4581	1	1
12	2.4050	11.5	11.5	13.8	2144.3875	1	1
13	2.6054	11.6	11.5	13.8	2144.3875	1.0087	1.0043
14	2.8058	11.9	11.7	12.3	1911.3019	1.0171	1.0261
15	3.0063	12.3	11.9	11.9	1849.1458	1.0336	1.0522
16	3.2067	12.6	12	11.5	1786.9896	1.0500	1.0696
17	3.4071	12.9	12.2	11.5	1786.9896	1.0574	1.0913
18	3.6075	13.2	12.3	11.5	1786.9896	1.0732	1.1087

Table A.31: variation of pressure drop with superficial gas velocity for 40:30:30 mixture with $h_s=8.5\text{cm}$ and $\alpha=11.2^\circ$.

Flow rate (m^3/hr)	Gas velocity (m/sec)	h_{\max} (cm)	h_{\min} (cm)	ΔP (cm)	ΔP (N/m^2)	r	R
9	1.8038	8.5	8.5	6	932.3424	1	1
10	2.0042	8.5	8.5	6.7	1041.1157	1	1
11	2.2046	8.5	8.5	7.7	1196.5061	1	1
12	2.4050	8.5	8.5	8.8	1367.4355	1	1
13	2.6054	8.6	8.5	8	1243.1232	1.0118	1.0059
14	2.8058	8.8	8.6	8.2	1274.2013	1.0233	1.0235
15	3.0063	9.3	8.8	8.4	1305.2794	1.0568	1.0647
16	3.2067	10.1	9	8.4	1305.2794	1.1222	1.1235
17	3.4071	10.8	9.3	8.4	1305.2794	1.1613	1.1824
18	3.6075	11.8	9.6	8.4	1305.2794	1.2292	1.2588

Table A.32: variation of pressure drop with superficial gas velocity for 40:30:30 mixture with $h_s=9.5\text{cm}$ and $\alpha=11.2^\circ$.

Flow rate (m^3/hr)	Gas velocity (m/sec)	h_{\max} (cm)	h_{\min} (cm)	ΔP (cm)	ΔP (N/m^2)	r	R
9	1.8038	9.5	9.5	6.1	947.8814	1	1
10	2.0042	9.5	9.5	6.6	1025.5766	1	1
11	2.2046	9.5	9.5	7.8	1212.0451	1	1
12	2.4050	9.5	9.5	9.4	1460.6698	1	1
13	2.6054	9.5	9.5	10.5	1631.5992	1	1
14	2.8058	9.6	9.5	9.7	1507.2869	1.0105	1.0053
15	3.0063	9.9	9.7	9.9	1538.3650	1.0206	1.0316
16	3.2067	10.2	9.9	10	1553.9040	1.0303	1.0579
17	3.4071	11.5	10.4	10	1553.9040	1.1058	1.1526
18	3.6075	12.2	10.6	10	1553.9040	1.1509	1.2000

Table A.33: variation of pressure drop with superficial gas velocity for 40:30:30 mixture with $h_s=10.5\text{cm}$ and $\alpha=11.2^\circ$.

Flow rate (m^3/hr)	Gas velocity (m/sec)	h_{\max} (cm)	h_{\min} (cm)	ΔP (cm)	ΔP (N/m^2)	r	R
9	1.8038	10.5	10.5	6.3	978.9595	1	1
10	2.0042	10.5	10.5	7.1	1103.2718	1	1
11	2.2046	10.5	10.5	8.2	1274.2013	1	1
12	2.4050	10.5	10.5	9.5	1476.2088	1	1
13	2.6054	10.5	10.5	11.1	1724.8334	1	1
14	2.8058	10.6	10.5	10.5	1631.5992	1.0095	1.0048
15	3.0063	10.8	10.6	10.5	1631.5992	1.0189	1.0190
16	3.2067	11.2	10.8	10.7	1662.6773	1.0370	1.0476
17	3.4071	12.2	11.3	10.7	1662.6773	1.0796	1.1190
18	3.6075	13	11.6	10.7	1662.6773	1.1207	1.1714

Table A.34: Variation of pressure drop with superficial gas velocity for 40:30:30 mixture with $h_s=11.5\text{cm}$ and $\alpha=11.2^\circ$.

Flow rate (m^3/hr)	Gas velocity (m/sec)	h_{\max} (cm)	h_{\min} (cm)	ΔP (cm)	ΔP (N/m^2)	r	R
9	1.8038	11.5	11.5	6.7	1041.1157	1	1
10	2.0042	11.5	11.5	7.4	1149.8890	1	1
11	2.2046	11.5	11.5	8.7	1351.8965	1	1
12	2.4050	11.5	11.5	9.9	1538.3650	1	1
13	2.6054	11.5	11.5	11.2	1740.3725	1	1
14	2.8058	11.5	11.5	11.8	1833.6067	1	1
15	3.0063	11.6	11.5	11.6	1802.5286	1.0087	1.0043
16	3.2067	11.9	11.7	11.6	1802.5286	1.0171	1.0261
17	3.4071	12.7	12.1	11.6	1802.5286	1.0496	1.0783
18	3.6075	13.3	12.3	11.6	1802.5286	1.0813	1.1130

Table A.35: variation of pressure drop with superficial gas velocity for 33.3:33.3:33.3 mixture with $h_s=8.5\text{cm}$ and $\alpha=11.2^0$.

Flow rate (m^3/hr)	Gas velocity (m/sec)	h_{\max} (cm)	h_{\min} (cm)	ΔP (cm)	ΔP (N/m^2)	r	R
9	1.8038	8.5	8.5	5.8	901.2643	1	1
10	2.0042	8.5	8.5	6.5	1010.0376	1	1
11	2.2046	8.5	8.5	7.8	1212.0451	1	1
12	2.4050	8.5	8.5	9.3	1445.1307	1	1
13	2.6054	8.6	8.5	8.6	1336.3574	1.0118	1.0059
14	2.8058	8.9	8.7	8.8	1367.4355	1.0230	1.0353
15	3.0063	9.4	8.9	8.8	1367.4355	1.0562	1.0765
16	3.2067	10.3	9.2	8.8	1367.4355	1.1196	1.1471
17	3.4071	11.3	9.6	8.8	1367.4355	1.1771	1.2294
18	3.6075	11.9	10.1	8.8	1367.4355	1.1782	1.2941

Table A.36: variation of pressure drop with superficial gas velocity for 33.3:33.3:33.3 mixture with $h_s=9.5\text{cm}$ and $\alpha=11.2^0$.

Flow rate (m^3/hr)	Gas velocity (m/sec)	h_{\max} (cm)	h_{\min} (cm)	ΔP (cm)	ΔP (N/m^2)	r	R
9	1.8038	9.5	9.5	6	932.3424	1	1
10	2.0042	9.5	9.5	6.4	994.4986	1	1
11	2.2046	9.5	9.5	7.4	1149.8890	1	1
12	2.4050	9.5	9.5	8.8	1367.4355	1	1
13	2.6054	9.5	9.5	9.8	1522.8259	1	1
14	2.8058	9.7	9.6	9.7	1507.2869	1.0104	1.0158
15	3.0063	9.8	9.7	9.6	1491.7478	1.0103	1.0263
16	3.2067	10.6	10	9.6	1491.7478	1.0600	1.0842
17	3.4071	11.6	10.4	9.6	1491.7478	1.1154	1.1579
18	3.6075	12.7	11	9.6	1491.7478	1.1545	1.2474

Table A.37: variation of pressure drop with superficial gas velocity for 33.3:33.3:33.3 mixture with $h_s=10.5\text{cm}$ and $\alpha=11.2^\circ$.

Flow rate (m^3/hr)	Gas velocity (m/sec)	h_{\max} (cm)	h_{\min} (cm)	ΔP (cm)	ΔP (N/m^2)	r	R
9	1.8038	10.5	10.5	6.1	947.8814	1	1
10	2.0042	10.5	10.5	7	1087.7328	1	1
11	2.2046	10.5	10.5	8.3	1289.7403	1	1
12	2.4050	10.5	10.5	9.7	1507.2869	1	1
13	2.6054	10.5	10.5	11.3	1755.9115	1	1
14	2.8058	10.6	10.5	10.5	1631.5992	1.0095	1.0048
15	3.0063	11	10.7	10.6	1647.1382	1.0280	1.0333
16	3.2067	11.7	10.9	10.5	1631.5992	1.0734	1.0762
17	3.4071	12.2	11.3	10.5	1631.5992	1.0796	1.1190
18	3.6075	12.5	11.4	10.5	1631.5992	1.0965	1.1381

Table A.38: variation of pressure drop with superficial gas velocity for 33.3:33.3:33.3 mixture with $h_s=11.5\text{cm}$ and $\alpha=11.2^\circ$.

Flow rate (m^3/hr)	Gas velocity (m/sec)	h_{\max} (cm)	h_{\min} (cm)	ΔP (cm)	ΔP (N/m^2)	r	R
9	1.8038	11.5	11.5	6.3	978.9595	1	1
10	2.0042	11.5	11.5	7	1087.7328	1	1
11	2.2046	11.5	11.5	8.3	1289.7403	1	1
12	2.4050	11.5	11.5	9.7	1507.2869	1	1
13	2.6054	11.5	11.5	11.3	1755.9115	1	1
14	2.8058	11.5	11.5	12.9	2004.5362	1	1
15	3.0063	11.7	11.6	11.8	1833.6067	1.0086	1.0130
16	3.2067	12.3	11.8	11.8	1833.6067	1.0424	1.0478
17	3.4071	12.8	12.1	11.8	1833.6067	1.0579	1.0826
18	3.6075	13.3	12.5	11.8	1833.6067	1.0640	1.1217

Table A.39: variation of pressure drop with superficial gas velocity for 20:60:20 mixture with $h_s=8.5\text{cm}$ and $\alpha=11.2^\circ$.

Flow rate (m^3/hr)	Gas velocity (m/sec)	h_{\max} (cm)	h_{\min} (cm)	ΔP (cm)	ΔP (N/m^2)	r	R
9	1.8038	8.5	8.5	5.8	901.2643	1	1
10	2.0042	8.5	8.5	6.4	994.4986	1	1
11	2.2046	8.5	8.5	7.3	1134.3499	1	1
12	2.4050	8.5	8.5	8.9	1382.9746	1	1
13	2.6054	8.7	8.6	8.7	1351.8965	1.0116	1.0176
14	2.8058	9.1	8.8	8.7	1351.8965	1.0341	1.0529
15	3.0063	9.6	9.1	8.8	1367.4355	1.0549	1.1000
16	3.2067	10.3	9.4	8.8	1367.4355	1.0957	1.1588
17	3.4071	11.5	9.7	8.8	1367.4355	1.1856	1.2471
18	3.6075	12.2	10.1	8.8	1367.4355	1.2079	1.3118

Table A.40: variation of pressure drop with superficial gas velocity for 20:60:20 mixture with $h_s=9.5\text{cm}$ and $\alpha=11.2^\circ$.

Flow rate (m^3/hr)	Gas velocity (m/sec)	h_{\max} (cm)	h_{\min} (cm)	ΔP (cm)	ΔP (N/m^2)	r	R
9	1.8038	9.5	9.5	5.9	916.8034	1	1
10	2.0042	9.5	9.5	6.6	1025.5766	1	1
11	2.2046	9.5	9.5	7.9	1227.5842	1	1
12	2.4050	9.5	9.5	9.4	1460.6698	1	1
13	2.6054	9.6	9.5	9.2	1429.5917	1.0105	1.0053
14	2.8058	9.8	9.6	9.2	1429.5917	1.0208	1.0211
15	3.0063	10.1	9.8	9.2	1429.5917	1.0306	1.0474
16	3.2067	10.7	10.1	9.2	1429.5917	1.0594	1.0947
17	3.4071	11.6	10.5	9.2	1429.5917	1.1048	1.1632
18	3.6075	12.3	11	9.2	1429.5917	1.1182	1.2263

Table A.41: variation of pressure drop with superficial gas velocity for 20:60:20 mixture with $h_s=10.5\text{cm}$ and $\alpha=11.2^\circ$.

Flow rate (m^3/hr)	Gas velocity (m/sec)	h_{\max} (cm)	h_{\min} (cm)	ΔP (cm)	ΔP (N/m^2)	r	R
9	1.8038	10.5	10.5	6.1	947.8814	1	1
10	2.0042	10.5	10.5	6.8	1056.6547	1	1
11	2.2046	10.5	10.5	7.6	1180.9670	1	1
12	2.4050	10.5	10.5	9.6	1491.7478	1	1
13	2.6054	10.5	10.5	10.3	1600.5211	1	1
14	2.8058	10.7	10.6	10.1	1569.4430	1.0094	1.0143
15	3.0063	11	10.7	10.1	1569.4430	1.0280	1.0333
16	3.2067	11.7	11	10.1	1569.4430	1.0636	1.0810
17	3.4071	12.1	11.3	10.1	1569.4430	1.0708	1.1143
18	3.6075	12.9	11.7	10.1	1569.4430	1.1026	1.1714

Table A.42: variation of pressure drop with superficial gas velocity for 20:60:20 mixture with $h_s=11.5\text{cm}$ and $\alpha=11.2^\circ$.

Flow rate (m^3/hr)	Gas velocity (m/sec)	h_{\max} (cm)	h_{\min} (cm)	ΔP (cm)	ΔP (N/m^2)	r	R
9	1.8038	11.5	11.5	6.3	978.9595	1	1
10	2.0042	11.5	11.5	7	1087.7328	1	1
11	2.2046	11.5	11.5	8.2	1274.2013	1	1
12	2.4050	11.5	11.5	9.9	1538.3650	1	1
13	2.6054	11.5	11.5	11.4	1771.4506	1	1
14	2.8058	11.6	11.5	11.2	1740.3725	1.0087	1.0043
15	3.0063	11.8	11.6	11.4	1771.4506	1.0172	1.0174
16	3.2067	12.2	11.8	11.2	1740.3725	1.0339	1.0435
17	3.4071	13.1	12.1	11	1709.2944	1.0826	1.0957
18	3.6075	13.7	12.5	11	1709.2944	1.0960	1.1391

Table A.43: variation of pressure drop with superficial gas velocity for 20:20:60 mixture with $h_s=8.5\text{cm}$ and $\alpha=11.2^\circ$.

Flow rate (m^3/hr)	Gas velocity (m/sec)	h_{\max} (cm)	h_{\min} (cm)	ΔP (cm)	ΔP (N/m^2)	r	R
9	1.8038	8.5	8.5	6.3	978.9595	1	1
10	2.0042	8.5	8.5	7.1	1103.2718	1	1
11	2.2046	8.5	8.5	8.4	1305.2794	1	1
12	2.4050	8.6	8.5	8.2	1274.2013	1.0118	1.0059
13	2.6054	8.8	8.6	8.4	1305.2794	1.0233	1.0235
14	2.8058	9.5	8.8	8.4	1305.2794	1.0795	1.0765
15	3.0063	10.1	9.1	8.4	1305.2794	1.1099	1.1294
16	3.2067	11.1	9.5	8.4	1305.2794	1.1684	1.2118
17	3.4071	12	9.7	8.4	1305.2794	1.2371	1.2765
18	3.6075	12.6	10	8.4	1305.2794	1.2600	1.3294

Table A.44: variation of pressure drop with superficial gas velocity for 20:20:60 mixture with $h_s=9.5\text{cm}$ and $\alpha=11.2^\circ$.

Flow rate (m^3/hr)	Gas velocity (m/sec)	h_{\max} (cm)	h_{\min} (cm)	ΔP (cm)	ΔP (N/m^2)	r	R
9	1.8038	9.5	9.5	6.6	1025.5766	1	1
10	2.0042	9.5	9.5	7.4	1149.8890	1	1
11	2.2046	9.5	9.5	8.7	1351.8965	1	1
12	2.4050	9.5	9.5	9.2	1429.5917	1	1
13	2.6054	9.6	9.5	9	1398.5136	1.0105	1.0053
14	2.8058	10.1	9.7	8.8	1367.4355	1.0412	1.0421
15	3.0063	10.8	10	9	1398.5136	1.0800	1.0947
16	3.2067	11.6	10.4	9	1398.5136	1.1154	1.1579
17	3.4071	12.5	10.7	9	1398.5136	1.1682	1.2211
18	3.6075	13	11	9	1398.5136	1.1818	1.2632

Table A.45: variation of pressure drop with superficial gas velocity for 20:20:60 mixture with $h_s=10.5\text{cm}$ and $\alpha=11.2^0$.

Flow rate (m^3/hr)	Gas velocity (m/sec)	h_{\max} (cm)	h_{\min} (cm)	ΔP (cm)	ΔP (N/m^2)	r	R
9	1.8038	10.5	10.5	7.3	1134.3499	1	1
10	2.0042	10.5	10.5	8	1243.1232	1	1
11	2.2046	10.5	10.5	9.2	1429.5917	1	1
12	2.4050	10.5	10.5	11.2	1740.3725	1	1
13	2.6054	10.6	10.5	10.9	1693.7554	1.0095	1.0048
14	2.8058	10.9	10.7	10.7	1662.6773	1.0187	1.0286
15	3.0063	11.6	11	10.7	1662.6773	1.0545	1.0762
16	3.2067	12.2	11.3	10.7	1662.6773	1.0796	1.1190
17	3.4071	12.9	11.6	10.5	1631.5992	1.1121	1.1667
18	3.6075	13.7	12	10.5	1631.5992	1.1417	1.2238

Table A.46: variation of pressure drop with superficial gas velocity for 20:20:60 mixture with $h_s=11.5\text{cm}$ and $\alpha=11.2^0$.

Flow rate (m^3/hr)	Gas velocity (m/sec)	h_{\max} (cm)	h_{\min} (cm)	ΔP (cm)	ΔP (N/m^2)	r	R
9	1.8038	11.5	11.5	7.1	1103.2718	1	1
10	2.0042	11.5	11.5	8.1	1258.6622	1	1
11	2.2046	11.5	11.5	9.3	1445.1307	1	1
12	2.4050	11.5	11.5	11.3	1755.9115	1	1
13	2.6054	11.5	11.5	12.8	1988.9971	1	1
14	2.8058	11.7	11.6	11.8	1833.6067	1.0086	1.0130
15	3.0063	12.3	11.8	11.5	1786.9896	1.0424	1.0478
16	3.2067	12.8	12.1	11.5	1786.9896	1.0579	1.0826
17	3.4071	13.7	12.5	11.1	1724.8334	1.0960	1.1391
18	3.6075	14.3	12.9	11.1	1724.8334	1.1085	1.1826

Table A.47: Variation of pressure drop with superficial gas velocity for 40:30:30 mixture with $h_s=10\text{cm}$ and $\alpha=9.52^\circ$.

Flow rate (m^3/hr)	Gas velocity (m/sec)	h_{\max} (cm)	h_{\min} (cm)	ΔP (cm)	ΔP (N/m^2)	r	R
12	2.4050	10	10	14.4	2237.6218	1	1
14	2.8058	10	10	16.5	2563.9416	1	1
16	3.2067	10	10	18.2	2828.1053	1	1
18	3.6075	10	10	18.5	2874.7224	1	1
20	4.0083	10.2	10	18	2797.0272	1.0200	1.0100
22	4.4092	10.7	10.2	17.6	2734.8710	1.0490	1.0450
24	4.8100	11.8	10.9	17.4	2703.7930	1.0826	1.1350
26	5.2108	13.2	11	17.4	2703.7930	1.2000	1.2100

Table A.48: Variation of pressure drop with superficial gas velocity for 40:30:30 mixture with $h_s=12.5\text{cm}$ and $\alpha=9.52^\circ$.

Flow rate (m^3/hr)	Gas velocity (m/sec)	h_{\max} (cm)	h_{\min} (cm)	ΔP (cm)	ΔP (N/m^2)	r	R
12	2.4050	12.5	12.5	15.6	2424.0902	1	1
14	2.8058	12.5	12.5	18.7	2905.8005	1	1
16	3.2067	12.5	12.5	21.8	3387.5107	1	1
18	3.6075	12.5	12.5	22.4	3480.7450	1	1
20	4.0083	12.8	12.6	21	3263.1984	1.0159	1.0160
22	4.4092	13.4	12.9	20.7	3216.5813	1.0388	1.0520
24	4.8100	14.2	13.4	20.9	3247.6594	1.0597	1.1040
26	5.2108	15.9	13.8	21	3263.1984	1.1522	1.1880

Table A.49: Variation of pressure drop with superficial gas velocity for 40:30:30 mixture with $h_s=15.1\text{cm}$ and $\alpha=9.52^0$.

Flow rate (m^3/hr)	Gas velocity (m/sec)	h_{\max} (cm)	h_{\min} (cm)	ΔP (cm)	ΔP (N/m^2)	r	R
12	2.4050	15.1	15.1	17	2641.6368	1	1
14	2.8058	15.1	15.1	19.8	3076.7299	1	1
16	3.2067	15.1	15.1	23.7	3682.7525	1	1
18	3.6075	15.1	15.1	27.2	4226.6189	1	1
20	4.0083	15.1	15.1	28.4	4413.0874	1	1
22	4.4092	15.7	15.4	25.7	3993.5333	1.0195	1.0298
24	4.8100	16.5	15.6	25.8	4009.0723	1.0577	1.0629
26	5.2108	17.6	16	26	4040.1504	1.1000	1.1126

Table A.50: Variation of pressure drop with superficial gas velocity for 33.3:33.3:33.3 mixture with $h_s=10.5\text{cm}$ and $\alpha=9.52^0$.

Flow rate (m^3/hr)	Gas velocity (m/sec)	h_{\max} (cm)	h_{\min} (cm)	ΔP (cm)	ΔP (N/m^2)	r	R
12	2.4050	10.5	10.5	14.3	2222.0827	1	1
14	2.8058	10.5	10.5	16.7	2595.0197	1	1
16	3.2067	10.5	10.5	17.9	2781.4882	1	1
18	3.6075	11.1	10.7	16.8	2610.5587	1.0381	1.0374
20	4.0083	11.8	11	15.4	2393.0122	1.0857	1.0727
22	4.4092	12.7	11.3	15.1	2346.3950	1.1429	1.1239
24	4.8100	13.9	11.9	14.9	2315.3170	1.2286	1.1681
26	5.2108	15.5	12.1	14.8	2299.7779	1.3143	1.2810

Table A.51: Variation of pressure drop with superficial gas velocity for 33.3:33.3:33.3 mixture with $h_s=12.3\text{cm}$ and $\alpha=9.52^0$.

Flow rate (m^3/hr)	Gas velocity (m/sec)	h_{\max} (cm)	h_{\min} (cm)	ΔP (cm)	ΔP (N/m^2)	r	R
12	2.4050	12.3	12.3	13.6	2113.3094	1	1
14	2.8058	12.3	12.3	14.7	2284.2389	1	1
16	3.2067	12.3	12.3	16.2	2517.3245	1	1
18	3.6075	12.8	12.4	15.8	2455.1683	1.0323	1.0244
20	4.0083	13.6	12.7	15.3	2377.4731	1.0709	1.0691
22	4.4092	15.1	13.3	15.1	2346.3950	1.1353	1.1545
24	4.8100	16.5	13.9	15	2330.8560	1.1871	1.2358
26	5.2108	17.1	14.2	14.9	2315.3170	1.2042	1.2724

Table A.52: Variation of pressure drop with superficial gas velocity for 33.3:33.3:33.3 mixture with $h_s=14.7\text{cm}$ and $\alpha=9.52^0$.

Flow rate (m^3/hr)	Gas velocity (m/sec)	h_{\max} (cm)	h_{\min} (cm)	ΔP (cm)	ΔP (N/m^2)	r	R
12	2.4050	14.7	14.7	13.7	2128.8485	1	1
14	2.8058	14.7	14.7	15.2	2361.9341	1	1
16	3.2067	14.7	14.7	18.1	2812.5662	1	1
18	3.6075	14.7	14.7	20.3	3154.4251	1	1
20	4.0083	14.7	14.7	21.8	3387.5107	1	1
22	4.4092	15.2	14.8	18.4	2859.1834	1.0270	1.0204
24	4.8100	16.4	15.2	17.2	2672.7149	1.0789	1.0748
26	5.2108	17.6	15.8	17	2641.6368	1.1139	1.1361

Table A.53: Variation of pressure drop with superficial gas velocity for 20:60:20 mixture with $h_s=10.5\text{cm}$ and $\alpha=9.52^0$.

Flow rate (m^3/hr)	Gas velocity (m/sec)	h_{\max} (cm)	h_{\min} (cm)	ΔP (cm)	ΔP (N/m^2)	r	R
12	2.4050	10.5	10.5	12	1864.6848	1	1
14	2.8058	10.5	10.5	14.8	2299.7779	1	1
16	3.2067	10.5	10.5	16.3	2532.8635	1	1
18	3.6075	10.8	10.6	15.4	2393.0122	1.0189	1.0190
20	4.0083	11.3	10.8	15.6	2424.0902	1.0463	1.0524
22	4.4092	11.9	11	15.5	2408.5512	1.0818	1.0905
24	4.8100	13.1	11.7	15.4	2393.0122	1.1197	1.1810
26	5.2108	14	11.9	15.1	2346.3950	1.1765	1.2333
28	5.6117	15.2	12.1	15.1	2346.3950	1.2562	1.3000

Table A.54: Variation of pressure drop with superficial gas velocity for 20:60:20 mixture with $h_s=12.1\text{cm}$ and $\alpha=9.52^0$.

Flow rate (m^3/hr)	Gas velocity (m/sec)	h_{\max} (cm)	h_{\min} (cm)	ΔP (cm)	ΔP (N/m^2)	r	R
12	2.4050	12.1	12.1	12.6	1957.9190	1	1
14	2.8058	12.1	12.1	14.4	2237.6218	1	1
16	3.2067	12.1	12.1	16.8	2610.5587	1	1
18	3.6075	12.1	12.1	19.1	2967.9566	1	1
20	4.0083	12.1	12.1	20.8	3232.1203	1	1
22	4.4092	12.6	12.2	17.3	2688.2539	1.0328	1.0248
24	4.8100	13	12.4	16.9	2626.0978	1.0484	1.0496
26	5.2108	13.7	12.6	16.7	2595.0197	1.0873	1.0868
28	5.6117	14.6	13.1	16.6	2579.4806	1.1145	1.1446

Table A.55: Variation of pressure drop with superficial gas velocity for 20:60:20 mixture with $h_s=14.7\text{cm}$ and $\alpha=9.52^\circ$.

Flow rate (m^3/hr)	Gas velocity (m/sec)	h_{\max} (cm)	h_{\min} (cm)	ΔP (cm)	ΔP (N/m^2)	r	R
12	2.4050	14.7	14.7	13.1	2035.6142	1	1
14	2.8058	14.7	14.7	14.9	2315.3170	1	1
16	3.2067	14.7	14.7	19.3	2999.0347	1	1
18	3.6075	14.7	14.7	20.7	3216.5813	1	1
20	4.0083	14.7	14.7	21.6	3356.4326	1	1
22	4.4092	15	14.7	18.5	2874.7224	1.0204	1.0102
24	4.8100	15.5	14.9	18.6	2890.2614	1.0403	1.0340
26	5.2108	16.3	15.3	18.7	2905.8005	1.0654	1.0748
28	5.611672278	17.4	15.6	18.5	2874.7224	1.1154	1.1224

Table A.56: Variation of pressure drop with superficial gas velocity for 20:20:60 mixture with $h_s=10.1\text{cm}$ and $\alpha=9.52^\circ$.

Flow rate (m^3/hr)	Gas velocity (m/sec)	h_{\max} (cm)	h_{\min} (cm)	ΔP (cm)	ΔP (N/m^2)	r	R
12	2.4050	10.1	10	12.1	1880.2238	1	1
14	2.8058	10.1	10	13.2	2051.1533	1	1
16	3.2067	10.1	10.5	14.4	2237.6218	1	1
18	3.6075	10.9	10.3	12.7	1973.4581	1.1262	1.0842
20	4.0083	11.6	10.6	13	2020.0752	1.1698	1.1386
22	4.4092	12.4	10.8	13.3	2066.6923	1.3056	1.2327
24	4.8100	14.1	11.2	13.2	2051.1533	1.4375	1.3515
26	5.2108	16.1	11.5	13.3	2066.6923	1.4000	1.3663

Table A.57: Variation of pressure drop with superficial gas velocity for 20:20:60 mixture with $h_s=12.4\text{cm}$ and $\alpha=9.52^\circ$.

Flow rate (m^3/hr)	Gas velocity (m/sec)	h_{\max} (cm)	h_{\min} (cm)	ΔP (cm)	ΔP (N/m^2)	r	R
12	2.4050	12.4	12.4	14.1	2191.0046	1	1
14	2.8058	12.4	12.4	16.2	2517.3245	1	1
16	3.2067	12.4	12.4	18.7	2905.8005	1	1
18	3.6075	12.4	12.4	21.1	3278.7374	1	1
20	4.0083	13.1	12.6	18.6	2890.2614	1.0397	1.0363
22	4.4092	13.8	12.9	17.5	2719.3320	1.0698	1.0766
24	4.8100	15.1	13.4	17.3	2688.2539	1.1269	1.1492
26	5.2108	17.3	13.9	17.2	2672.7149	1.2446	1.2581

Table A.58: Variation of pressure drop with superficial gas velocity for 20:20:60 mixture with $h_s=15.1\text{cm}$ and $\alpha=9.52^\circ$.

Flow rate (m^3/hr)	Gas velocity (m/sec)	h_{\max} (cm)	h_{\min} (cm)	ΔP (cm)	ΔP (N/m^2)	r	R
12	2.4050	15.1	15.1	19.2	2983.4957	1	1
14	2.8058	15.1	15.1	21.1	3278.7374	1	1
16	3.2067	15.1	15.1	24.2	3760.4477	1	1
18	3.6075	15.1	15.1	25.1	3900.2990	1	1
20	4.0083	15.1	15.1	26.5	4117.8456	1	1
22	4.4092	16.9	15.9	19.7	3061.1909	1.0629	1.0861
24	4.8100	17.6	16.2	18.4	2859.1834	1.0864	1.1192
26	5.2108	18.9	16.4	18.1	2812.5662	1.1524	1.1689